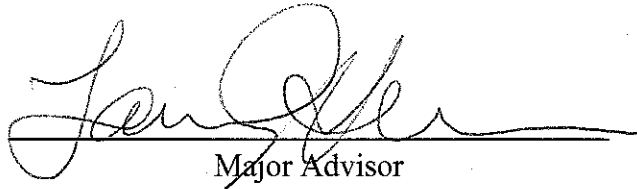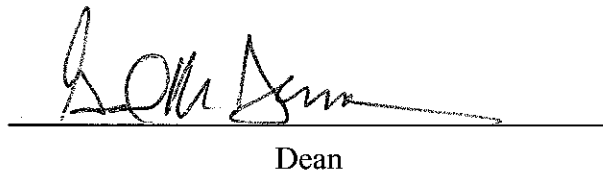Thesis Approved by:

_____
Major Advisor

_____
Dean

Erbb2: A Regulator of the Skin's Response to Ultraviolet Radiation

By

Rebecca Jangraw Ophardt

A THESIS

Submitted to the faculty of the Graduate School of the Creighton University

in Partial Fulfillment of the Requirements for the degree of

Master of Science in the Department of Biomedical Sciences

Omaha, NE

May 20, 2008

Abstract

Non-melanoma skin cancer is the most commonly diagnosed cancer in the United States. The cause of most non-melanoma skin cancer is prolonged exposure to UV-irradiation. UV-irradiation acts as both an initiator and tumor promoter, possibly through its activation of receptor tyrosine kinases (RTKs) such as the members of the Erbb family. Erbb2, an orphan receptor and member of the Erbb family, was recently demonstrated to be involved in the regulation of cell cycle progression after UV-induced DNA damage. This report describes the use of a skin-targeted conditional *Erbb2* null mouse (to be referred here as an *Erbb2* mutant mouse) to study Erbb2's role in the skin's response to UV-irradiation. Using this model, the effects of Erbb2 on cell cycle progression, DNA damage repair, and mutagenesis were analyzed after UV-irradiation. Surprisingly, *Erbb2* mutant skin lacks a UV-induced S-phase arrest observed in previous studies utilizing the Erbb2 inhibitor AG825, suggesting that *Erbb2* mutant skin compensates for its loss of Erbb2. However, Erbb2 reduces the efficiency of DNA damage repair and increases clonal expansion of keratinocytes with *Trp53* mutations through mechanisms independent of its regulation of the cell cycle after UV-irradiation. These results suggest that erbb2 may contribute to skin carcinogenesis through multiple mechanisms.

Dedication

This thesis is dedicated to my husband, Jon, whose unconditional love, patience, and support, even from a different state, were instrumental in helping me complete this work. This thesis is also dedicate this to my parents, who taught me that anything is possible and made me determined to achieve my goals. To my father, who has always challenged me to think and not always take the easy route. And, to my mother, my friend, who's enduring patience, strength, and wisdom have been and continue to be invaluable to me.

Acknowledgements

My sincere thanks to my advisor, Dr. Laura Hansen, for her mentoring and guidance. Thank you for having confidence in me and for teaching me to think like a scientist. This thesis would also not have been possible without the members of the Hansen Lab, especially Jodi Nicolai, David Lynch, Kyle Bischel, Andrew Bowles, Jackie Evenson, Jodi Yanagida, Jennifer Correia, and Jessica Gaulter. I am grateful for their contributions to my research and this experience would not have been nearly as much fun without them. (Go Team Hansen!) Lastly, I extend my thanks to Dr. Greg Perry in the Flow Cytometry Core Facility, who was instrumental in collecting data from my samples and who provided wonderful troubleshooting advice.

Table of Contents

List of Figures and Tables

Figure Contributions

Jennifer Correia	p53 and BrdU-labeling index quantification (Figure 9B and Figure 12B and C)
Dr. Laura Hansen	Cyclobutane dimer quantification and photograph of *Erbb2* mutant mouse (Figure 5C and Figure 11A)
David Lynch	*In vitro* flow cytometry (*Erbb2* mutant and control, Figure 13)
Justin Madson	Immunoblotting of phospho-Erbb2 (mouse keratinocytes, Figure 7B, reprinted from Am J Pathol 2006;169:1402-1414 with permission from the American Society for Investigative Pathology)
Jodi Nicolai	Erbb2 immunoblotting and quantification in *Erbb2* mutant skin and immunoblotting of phospho-Erbb2 in UV-exposed human skin (Figure 5B and Figure 7A)
Jodi Yanagida	Photographs of BrdU immunofluorescence (Figure 9A)

Abbreviations

Abbreviation **Description**

2MED   Twice the minimal erythema dose

ATR   Ataxia telangiectasia mutated and Rad3 related

a.u.   Arbitrary Unit

BCC   Basal Cell Carcinoma

BrdU   Bromodeoxyuridine

C   Cytosine

CBD   Cyclobutane dimers

CDK   Cyclin dependent kinase

DMBA   Di-methyl-benzanthracene

EGFR   Epidermal Growth Factor Receptor

G_o/G_1 Gap 0 / Gap 1 Phases

G_2/M Gap 2 / Mitosis Phases

GAPDH   Glyceraldehyde 3-Phosphate Dehydrogenase

h   Hour(s)

HER2   Human EGF receptor 2

K14   Keratin 14

kDa   Kilodalton

min   Minute(s)

PBS   Phosphate buffered saline

PCNA   Proliferating cell nuclear antigen

PI3K   Phosphatidyl-inisitol 3-kinase

PKC	Protein kinase C
PLC	Phospholipase C
PTB	Phosphotyrosine binding
PTP	Protein tyrosine phosphatase
RTK	Receptor Tyrosine Kinase
ROS	Reactive Oxygen Species
SCC	Squamous Cell Carcinoma
SDS-PAGE	Sodium Dodecyl Sulfate Polyacrylamide Gel Electrophoresis
SH2	*src* homology-2
T	Thymine
TPA	12-O-tetradecanoylphorbol-13-acetate
UV	Ultraviolet

Chapter 1: Introduction

The skin is our barrier from the elements

The skin is a complex organ containing several different layers, structures, and cell types. It protects the body from environmental insults, small molecules, and water loss. The skin is comprised of three layers; from the outer-most layer they are: the epidermis, the dermis, and the subcutaneous layer. The epidermis is mostly (>90%) keratinocytes with other cell types such as melanocytes (pigment cells), Langerhans cells (antigen-presenting cells), and Merkel cells (neuroendocrine cells, also found in the dermis). Interior to the epidermis is the basement membrane which separates the keratinocytes from the dermis. The dermis, which consists mostly of collagen and elastic fibrils and fibroblastic cells, contains structures such as hair follicles and sweat glands. The subcutaneous layer lies underneath the dermis, consists mainly of adipose tissue and connects the skin to underlying muscle and bone. Nerve fibers exist in all three skin layers with blood vessels present to provide nutrients and remove waste from the dermal and subcutaneous layers.

The keratinocytes in the epidermis form a keratinized stratified squamous epithelium. The layers of the stratified epithelium are, from the basement membrane, the stratum basale, stratum spinosum, stratum granulosum, stratum lucidum (sometimes present), and stratum corneum. The cells in the basal layer, or stratum basale, are columnar shaped keratinocytes that rapidly undergo asymmetric cell divisions and promote stratification and differentiation (1). Over time, these cells change in phenotype and protein expression profiles and migrate toward the skin's surface. As this migration

occurs, the cells become more rounded and granular, then squamous, and are eventually

shed or lost due to environmental stresses. The terminally differentiated cells of the

stratum corneum are considered 'dead cells' as they are anucleate. They are replaced as

additional cells migrate upwards. In this way, the skin maintains homeostasis.

UV irradiation causes DNA damage, the repair of which is facilitated by cell cycle arrest

As the interface with the outside world and barrier from the elements, the skin

sustains damage from and responds to outside stimuli such as ultraviolet (UV) irradiation.

UV makes up 10% of the total solar radiation that reaches the earth and can be divided

into three categories, based on wavelength. These are, in order of increasing energy and

decreasing penetration: UVA (320-400 nm), UVB (280-320 nm), and UVC (200-280

nm). UVC and part of UVB are filtered out by the atmosphere and therefore never reach

the earth except in areas where the ozone is depleted. Therefore, the solar radiation that

reaches the earth is mostly UVA (~90%) and some UVB (~10%).

UVA and UVB both cause DNA damage through different mechanisms. UVA

penetrates into the epidermis and the top layers of the dermis causing DNA damage

indirectly through the creation of reactive oxygen species (ROS). UVB causes damage

directly in the epidermis through DNA absorption. UVB is considered to be more

carcinogenic than UVA (2).

The major forms of UV-induced DNA damage caused by ROS or UVB

absorption are DNA photoproducts (i.e. cyclobutane dimers and 6-4 photoproducts).

DNA photoproducts are bulky adducts that result from bonds formed between adjacent

pyrimidine bases. DNA photoproducts resulting from UV-irradiation are repaired through

nucleotide excision repair. In this process, DNA is repaired by several factors involved in (i) recognition of DNA damage, (ii) cleavage of the DNA several nucleotides of each side of the adduct, (iii) removal of the damaged oligomer, (iv) recruitment of polymerase machinery to fill in the gap, and (v) ligation (3).

One way that UV-induced DNA damage is recognized and nucleotide excision repair is facilitated is though the ataxia telangiectasia mutated and Rad3 related (ATR) pathway (Figure 1A, (4)). ATR is recruited to sites of DNA damage recognition proteins (5;6). ATR then phosphorylates the activating phosphorylation sites on the Chk1 kinase (5;7), which phosphorylates Cdc25A and targets it for ubiquitin-dependent degradation (8;9). The members of the Cdc25 family (Cdc25A, Cdc25B, and Cdc25C) are phosphatases responsible for dephosphorylating the inhibitory phosphorylation sites on cyclin dependent kinases 1 and 2 (CDK1, CDK2), resulting in their activation. The activation of CDK-cyclin complexes regulates progression through each phase of the cell cycle (Figure 1B). Cdc25A normally activates CDK2, allowing progression through the G_1- and S-phase regulatory checkpoints (10), while Cdc25B/C are involved in the activation of the CDK1-cyclin B complex and the entry into mitosis (11-13). When Cdc25A is degraded in response to UV-induced DNA damage, cyclin/CDK2 complexes are inhibited and cells accumulate in S-phase (7;14). Cell cycle arrest allows time for DNA damage to be assessed and for nucleotide excision repair-related proteins to remove DNA damage and facilitate replication (3). Or, if DNA damage is too extensive, the cell(s) can undergo apoptosis (reviewed in (15)).
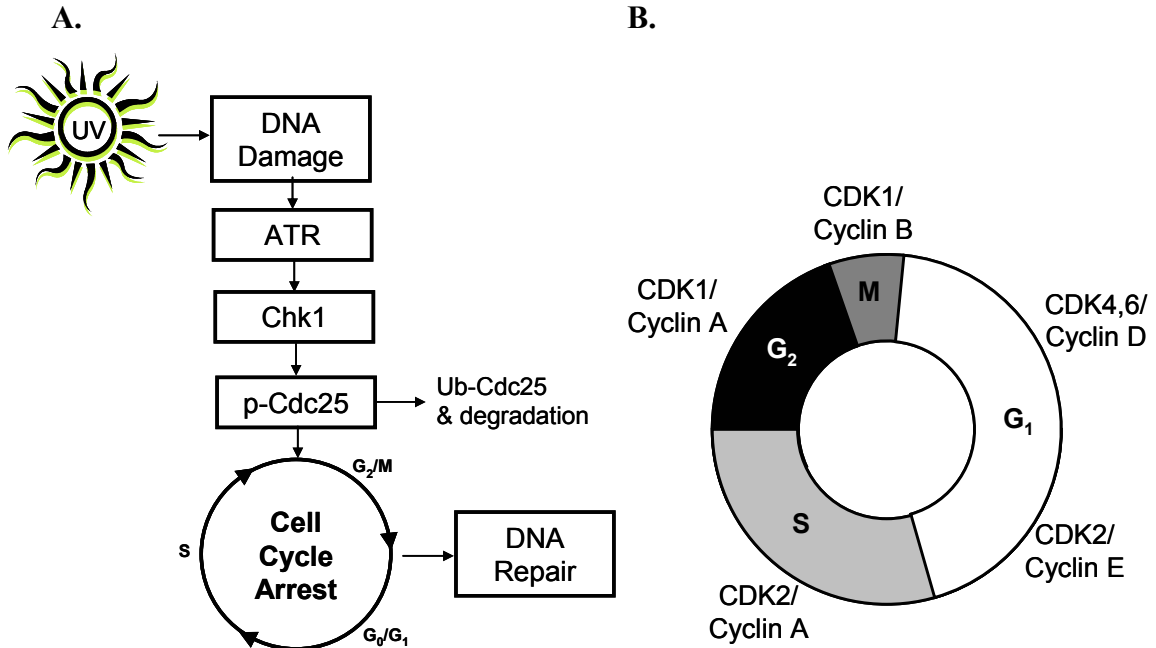
Figure 1. ATR pathway activation results in cell cycle arrest through Cdc25A degradation.

A. UV-induced DNA damage results in activation of the ATR pathway. Degradation of Cdc25A/B/C phosphatases results in a cell cycle arrest by inactivation of CDK1/2. B. Activation of different cyclin-CDK complexes are necessary for progression through each phase of the cell cycle.

Insufficient DNA damage repair results in mutagenesis, the most common of which is **Trp53** *mutation*

Hallmark mutations of UV-induced DNA damage, C→T or CC→TT transitions occur mainly at pyrimidine dimers (16). These transitions most commonly occur at CpG (5'-CG-3') sequences where cytosines can be spontaneously deaminated or preferentially targeted by carcinogens (17-19).

Mutations of *Trp53*, the gene that encodes for the p53 tumor suppressor, are the most common and earliest known mutations in non-melanoma skin cancer, occurring in between 12-58% of SCC and BCC (20). p53 is a transcription factor that regulates the expression of many different genes involved in cell-cycle arrest, apoptosis, senescence,

DNA repair, and angiogenesis. It also stimulates an autoregulatory negative feedback loop by promoting transcription of Mdm2, a negative regulator of p53. Mdm2 exports p53 from the nucleus, and acts as an E3 ligase, targeting p53 for proteasomal degradation (reviewed in (21)).

The most common *Trp53* mutations in UV-exposed skin are UV signature mutations (22;23) in the DNA binding region, resulting in a dominant negative mutant p53 with an increased half-life (24-29). Dominant negative mutant p53 blocks transcription factor activity of wild type p53 (21), depriving cells of its important tumor suppressor function and increasing cancer risk.

UV irradiation causes skin cancer

The major cause of non-melanoma skin cancer is exposure to UV-irradiation. Non-melanoma skin cancer is the most prevalent cancer in the United States and the National Cancer Institute (NCI) estimates that in 2007 over one million new cases of non-melanoma skin cancers were diagnosed in the United States and less than 2,000 (<1% new diagnosed cases) deaths could be contributed to non-melanoma skin cancers (http://www.cancer.gov/cancertopics/types/skin). Though non-melanoma skin cancers are not commonly life threatening, they are among the most costly to treat due to their high incidence (30). In 2001, Chen, et al. estimated the cost for non-melanoma skin cancer treatment at $650 million for the entire United States' population (31). The majority (70-80%) of diagnosed non-melanoma skin cancer cases are basal cell carcinomas (BCC). BCC cells have the columnar phenotype of the cells in the basal layer of the epidermis. The other type of non-melanoma skin cancer is squamous cell

carcinoma (SCC) which, like the keratinocytes in the stratus corneum, has a more squamous phenotype. Both BCC and SCC arise from keratinocytes in the skin.

Carcinogenesis generally follows the multistage tumorigenesis model (Figure 2, (32;33)). If UV-induced DNA damage is not correctly repaired, a genetic mutation can become fixed resulting in an initiated cell. This cell undergoes clonal expansion through the addition of growth stimuli and becomes a benign tumor. Additional gene mutations can result in the formation of a malignant and eventually metastatic tumor. UV-irradiation is capable of both causing DNA damage, which can lead to an initiated cell, and providing growth stimuli through multiple mechanisms (34-37).
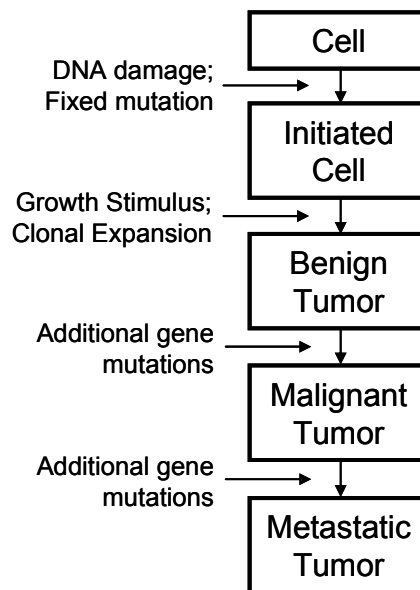
Figure 2. The multistage tumorigenesis model.
Schematic representation of multistage tumorigenesis model. UV-irradiation can result in both mutagenesis and growth stimuli, thereby promoting skin tumorigenesis.

SCC develop through the model described above but BCC are thought to develop through a slightly modified version of the multistage tumorigenesis model. BCC appear to develop into a malignant tumor directly from an initiated cell. Both BCC and SCC

have low rates of metastasis. However, immunosuppressed patients (i.e. transplant recipients) have increased rates of BCC (10 times) and SCC incidence (up to 250 times that of the normal population) as well as increased rates of recurrence and SCC metastasis (5-8%, reviewed in (38)).

UV irradiation indirectly activates receptor tyrosine kinases, including Erbb family members

One way that UV-irradiation stimulates proliferation is through activation of receptor tyrosine kinases (RTKs). RTKs such as members of the Erbb family, are indirectly activated by UV-irradiation through the inhibition of protein tyrosine phosphatases by reactive oxygen species (ROS) (39;40). Protein tyrosine phosphatases (PTPs) normally maintain low levels of receptor phosphorylation. ROS oxidize a critical cysteine residue in the active site of PTPs resulting in their inactivation and increased RTK activation (Figure 3, (41)). The aberrant activation of members of the Erbb family by UV-irradiation can result in an increase of tumor promoting growth stimuli. Mitogenic ligands (i.e. TGFα) that activate the Erbb receptors result in increased mRNA levels of membrane-bound ligand precursors (42). In addition, UV can stimulate the processing of TGFα from membrane-bound precursors through the activation of cell surface proteases (43;44). In this way UV promotes autocrine signalling by the Erbb family through a positive feedback loop (Figure 3).
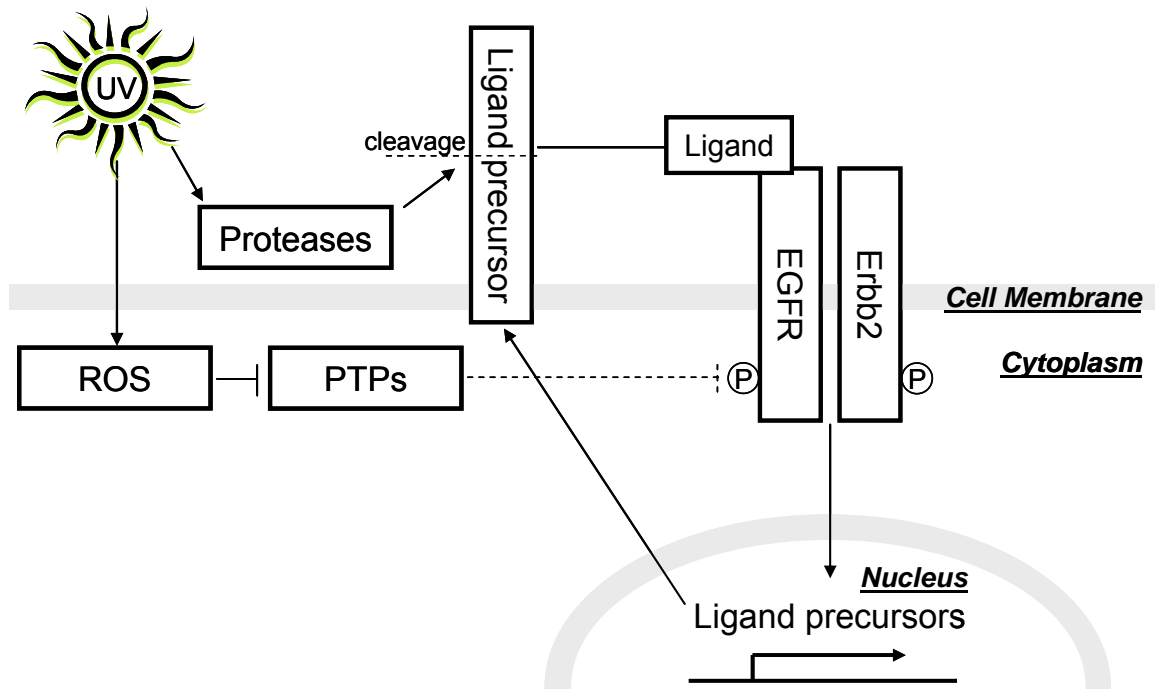
Figure 3. UV regulation of Erbb phosphorylation and autocrine signaling.
Schematic representation of UV regulation of Erbb family activation (i.e. EGFR, Erbb2) and growth stimuli through the deactivation of protein tyrosine phosphatases (PTPs) by ROS and the activation of proteases which enhance autocrine signaling through cleavage of membrane-bound ligand precursors.

Erbb2 is a member of the Erbb family of RTKs

One member of the Erbb family of RTKs that is activated by UV-irradiation is Erbb2. In 1985, *Erbb2* was isolated from DNA from rat neuroblastomas and was known to code for tumor antigen p185, termed NEU (45). It was shown that NEU had homology to, but was not derived from, Erbb, or epidermal growth factor receptor (EGFR), and was therefore named Human EGF receptor 2 (HER2) (46). Also in 1985, Semba, et al. discovered an Erbb-like gene (47) with protein tyrosine kinase activity (48) which was named Erbb2. In 1987 Di Fiore, et al. showed that *neu* is the rat homolog of human *erbB-2* by comparing sequences and chromosomal mappings (49).

The Erbb family of receptor tyrosine kinases is made up of four members: EGFR, Erbb2, Erbb3, and Erbb4, which are expressed in tissues of epithelial, mesenchymal and neuronal origin (50). Each of these members has a single transmembrane domain, an extracellular binding domain, and a cytoplasmic protein tyrosine kinase domain (51). Activation of these receptors begins with the binding of a ligand to the extracellular domain. Ligands that bind to the Erbb family of receptors are referred to as epidermal growth factor (EGF)-related peptide growth factors that are processed from transmembrane precursors (44). These growth factors include EGF, amphiregulin (AR), transforming growth factor- α (TGF-α), betacellulin (BTC), heparin-binding EGF (HB-EGF), epiregulin (EPR), and neuregulins (NRG) all of which have different receptor specificities (summarized in Table 1). The binding of a ligand to the extracellular domain directs the receptor to undergo homo- or hetero-dimerization with another member of the Erbb family. Dimerization of receptors results in auto- or trans-phosphorylation of the intracellular tyrosine kinase domain. Each receptor has multiple sites which are phosphorylated based on both the ligand and dimerization partner. After dimerization occurs, adaptor proteins that contain either Src homology-2 (SH2) or phosphotyrosine binding domains (PTB) are recruited to the phosphorylated receptors. The adapter protein(s) recruited depends on the location of the phosphorylation site and therefore, different ligand/receptor/phosphorylation site combinations lead to diversification of signal transduction.

The composition of homodimers is limited because Erbb3 has a defective kinase (52) and Erbb2 has no known ligand. Therefore, these receptors are reliant on heterodimerization with other Erbb family members to effectively trigger a signaling

cascade under normal conditions. Erbb2 is the preferred dimerization partner of all other Erbb family members and increases potency of signaling by enhancing the association with adapter proteins (53), decreasing ligand dissociation rates (54;55) and internalization (56), and increasing recycling of receptors that might otherwise be targeted for lysosomal degradation (57).

Table 1. Erbb family ligand specificity.

Receptor	Ligand
EGFR	EGF, AR, TGF-α
Erbb2	--
Erbb3 & Erbb4	NRG-1, NRG-2
Erbb4	NRG-3, NRG-4
EGFR & Erbb4	BTC, HB-EGF, EPR

Erbb2 regulates normal cellular processes

Erbb2 is involved in the activation of several signaling pathways that regulate normal cellular processes such as cell proliferation, survival, death, differentiation, adhesion, migration, inflammation, and angiogenesis (58;59). Signalling pathways activated by Erbb2 include phosphatidyl-inisitol 3-kinase (PI3K)/Akt, Ras-mitogen-activated protein kinase (MAPK), phospholipase C (PLC)-protein kinase C (PKC), Src, and Jak/Stat (reviewed in (60;61)). Upon activation of these signaling pathways, Erbb2 has an essential role in organ development and function. *Erbb2* null mice die midgestation (62), due to defects in cardiac and neuromuscular junctions (63;64). In 2002, Chan, et al. demonstrated that Erbb2 tyrosine kinase activity was necessary for both normal cardiac and neural development (65). Other studies have demonstrated that

Erbb2 is necessary for the prevention of dilated cardiomyopathy, a side effect of Erbb2-targeted therapeutics (66;67).

Erbb2 is a therapeutic target in a number of cancers

Erbb2 has been found to be overexpressed in a number of internal cancers, including, breast, colon, and ovarian cancers. Overexpression of Erbb2 in these cancers is generally indicative of aggressive cancer and a poor prognosis. Because of Erbb2's role in cancer development and progression, targeted therapies have been developed. These therapies include trastuzumab (Herceptin), a humanized Erbb2 monoclonal antibody targeted to the extracellular domain, and small molecule tyrosine kinase inhibitors (TKIs) which prevent receptor activation. The mechanism of action of trastuzumab is unknown, despite its widespread use. It has been suggested that trastuzumab prevents "shedding" of the extracellular domain of Erbb2 by proteolytic cleavage or decreases signaling by mediating internalization and degradation of the receptor (reviewed in (68)). Unfortunately, trastuzumab is only effective in about 30% of Erbb2-overexpressing breast cancers as a single agent. Though more effective when paired with chemotherapeutics, there is an increased risk for cardiotoxicity (69). In addition, some cancers acquire resistance against trastuzumab, limiting its use. Hsieh and Moasser (2007) suggest that due to incomplete inhibition of HER2 signaling, the potent HER2-HER3 heterodimer may still be able to potentiate growth signals through the PI3K/Akt pathway thereby making it necessary to develop more potent Erbb2-targeted TKIs (70). Clinical trials are currently underway for several small molecule inhibitors such as Lapatinib, a small molecule duel reversible inhibitor of EGFR (HER1) and HER2

tyrosine kinase activity. Lapatinib has shown promise when used in combination with trastuzumab and is currently in phase III clinical trials (reviewed in (68)).

Why study Erbb2's role in skin cancer?

EGFR, Erbb2, Erbb3, but not Erbb4 are expressed in the keratinocytes of the epidermis. In the basal keratinocytes of the epidermis, Erbb2 has a cytoplasmic localization, while in suprabasal keratinocytes it is localized to the cell surface (71;72). Several groups have reported dramatic phenotypes in Erbb-overexpressing transgenic mice, which include severe hyperplasia and spontaneous papilloma formation (73-76). There are conflicting results regarding Erbb2 protein levels in BCC and SCC (71;77), but Erbb2 mRNA and protein has been detected in human skin and non-melanoma skin cancers (78) and is activated upon UV-irradiation (Figure 7). Despite normal Erbb2 levels, UV-induced activation amplifies Erbb2's effects as an oncoprotein in the skin.

We recently demonstrated that UV-irradiation activates Erbb2 both *in vitro* and *in vivo* as measured by the phosphorylated receptor (79). Inhibition of Erbb2 using the tyrphostin inhibitor AG825 reduces DNA synthesis both in sham- and UV-irradiated keratinocytes (79). In addition, inhibition of Erbb2 causes S-phase arrest, during which the cells respond to and repair UV-induced DNA damage. Inhibition of Erbb2 in sham- and UV-irradiated keratinocytes also decreases Cdc25A immunoreactivity, suggesting that Erbb2 maintains Cdc25A levels. These results suggest that Erbb2 may regulate the ATR pathway.

Previously, it has been demonstrated that Akt phosphorylates Chk1 at serine 280, an inhibitory phosphorylation site (80;81). Since Chk1 targets Cdc25A for degradation resulting in an S-phase arrest, an inactive Chk1 would result in maintenance of Cdc25A

and S-phase progression after DNA damage. One of the signaling pathways that Erbb2 activates after UV-irradiation is the PI3K/Akt survival pathway. Therefore, Erbb2 is suspected to regulate the ATR pathway through the PI3K/Akt pathway. Through this mechanism, the UV-induced activation of Erbb2 could prevent the phosphorylation and degradation of Cdc25A and therefore prevent a cell cycle arrest and reduce the efficiency of DNA damage repair (Figure 4). However, it has not yet been determined whether Erbb2 regulates the ATR DNA damage pathway through this mechanism.
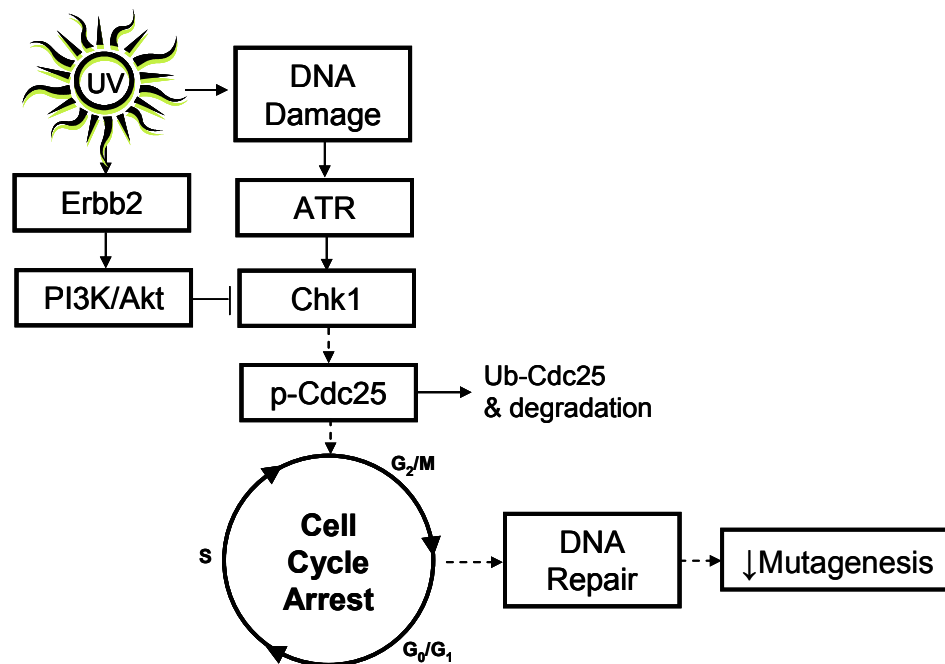
Figure 4. Potential mechanism for Erbb2 regulation of the ATR DNA damage response pathway.
Schematic representation of the potential mechanism in which Erbb2 might regulate the cell's response to UV-induced DNA damage. Erbb2 activates the PI3K/Akt pathway which may cause the deactivation of Chk1, ultimately preventing cell cycle arrest. The lack of cell cycle arrest reduces the efficiency of DNA damage repair and increases the probability of mutagenesis.

To determine whether S-phase arrest suppresses tumorigenesis, CD-1 mouse skin was treated with AG825 or DMSO (control) and was sham- and UV-irradiated (two

exposures totaling 20kJ/m^2). UV-irradiated DMSO-treated mice formed about twice as many tumors that were about twice the volume of the tumors formed in AG825-treated mice 12 weeks after the final UV exposure, suggesting that Erbb2 promotes UV-induced skin tumorigenesis. Although the tyrphostin inhibitor AG825 is about 60 times more specific for Erbb2 than EGFR (69;70), off-target effects make the inhibition of Erbb2 by AG825 an imperfect system for studying the function of Erbb2. Therefore, a skin-targeted conditional *Erbb2* null mouse model was developed to study Erbb2's involvement in the response of the skin to UV-irradiation.

Since cell cycle arrest increases the efficiency of DNA damage repair, we hypothesized that promotion of S-phase progression by Erbb2 after UV-irradiation limits DNA damage repair and results in increased mutagenesis. In order to test this hypothesis, *Erbb2* mutant and littermate controls were exposed repeatedly to UV-irradiation and euthanized prior to tumor development. The role of Erbb2 in the regulation of cell cycle progression, DNA damage repair, and mutagenesis was investigated. Genetic ablation of *Erbb2* in the skin results in a compensatory upregulation of Cdc25A which may have implications for the long term use of Erbb2-targeted therapeutics. This work also suggests that Erbb2 has a role in the regulation of UV-induced DNA damage repair and mutagenesis independent of its regulation of cell cycle progression.

Chapter 2: Materials and Methods

Animals

Erbb2 floxed (*Erbb2$^{fl/fl}$*) mice were generously provided by Dr. Ulrich Mueller (Scripps Institute, La Jolla, CA); *loxP* sites were inserted on either side of the first coding exon of *Erbb2* as described in (82). These mice were crossed with transgenic mice on an FVB/N background in which Cre recombinase expression was driven by the Keratin 14 promoter (K14 Cre) (The Jackson Laboratory, Bar Harbor, ME) to create *Erbb2* mutant mice (*Erbb2$^{fl/fl}$ cre$^+$*) and littermate controls (*Erbb2$^{fl/fl}$ cre$^-$*). All mice were maintained in the Creighton University Animal Facility and were fed with Purina lab chow (Nestlé Purina Pet Care, St. Louis, MO) and given water ad libitum. All animal procedures were performed in accordance with American Association of Laboratory Animal Care guidelines and approved by the institutional animal care and use committee (IACUC).

Keratinocyte Culture

Newborn pups were euthanized and sterilized with betadine and 70% ethanol. Skin was removed as described in (83) and floated on 0.25% trypsin (Invitrogen) with 10% versene (Invitrogen) overnight at 4ºC. The epidermis and dermis were separated. Epidermises from mice of the same genotype were pooled and minced using sterile scissors. Cells were plated in sterile polystyrene 60 mm dishes (Becton Dickinson) in minimum essential media (S-MEM, Invitrogen), containing 8% fetal bovine serum (FBS, Lifeblood Medical, Adelphia, NJ) and 1% Penicillin/Streptomycin (Invitrogen), referred to as HiCa medium. The day after plating and every two to three days thereafter, the cells were refed with S-MEM containing a mixture of unchelexed and chelexed FBS (Lifeblood

Medical) with a calcium concentration adjusted to 0.05 mM, and 1%

penicillin/streptomycin (Invitrogen), referred to as LoCa medium. Serum was chelexed

to reduce the calcium concentration using Chelex 100 Resin (Bio-Rad Laboratories,

Hercules CA). The calcium level of the FBS was measured by Dr. U. Lichti (NCI).

Ultraviolet Irradiation

Ultraviolet (UV) radiation was generated by Ultraviolet-B TL 40W/12 RS Bulbs (Philips,

Somerset, NJ), which emit approximately 30% UVA, 70% UVB, and <1% UVC, as

measured using Oriel Goldilux radiometric photodetector probes (Newport Corporation,

Irvine, CA). On the day of UV-irradiation, the hair on the dorsal skin was clipped using a

Wahl Animal Trimmer (Wahl Clipper Corporation, Sterling, IL) and shaved with a

microscreen wet/dry electric shaver (Panasonic, Kadoma, Osaka, Japan). Once shaved,

mice were placed under the UV bulbs, receiving between 0.5-3.0 kJ/m^2. Keratinocytes in

culture were covered with phosphate buffered saline (PBS) containing 0.05 mM $CaCl_2$

and were placed under the lamp, receiving 600 J/m^2 UV. Protein lysate from UV-

exposed human skin was generously provided by Dr. Gary Fisher (University of

Michigan, study 1087). Human skin was sham- or UVB-irradiated at twice the minimal

erythema dose (2MED, measured for each patient, ranging between 0.6 kJ/m^2 and 1.0

kJ/m^2) as described in (84).

Virus infection

Keratinocytes were cultured until they reached 60-70% confluency. The cells were

incubated with empty or Cre adenoviruses (a generous gift from Dr. Stuart Yuspa (NIH))

at 30 plaque forming units per cell (PFU/cell), in S-MEM with 4 μg/mL polybrene

(Sigma-Aldrich, St. Louis, MO) for 45 min. LoCa was added to the cells and virus

mixture. Cells were infected 24 h prior to UV-irradiation.

Experimental Design

Age matched *Erbb2* mutant mice and littermate controls (described above) were sham- or

UV-irradiated 43 times over 39 weeks as per the procedure described above. Mice in

UV- and sham-irradiated groups were injected with bromodeoxyuridine (BrdU, Sigma,

St. Louis, MO) 1 h prior to euthanization (approximately 2.25 mg per 30 g body weight).

Mice were euthanized 1, 12, 18, 36, or 72 h after the final UV exposure. Pieces of whole

skin were flash frozen on dry ice. Dorsal skin sections were also fixed in 70% ethanol or

10% buffered formalin. Paraffin embedded blocks and slides were prepared by American

Histolabs (Gaithersburg, MD).

Immunofluorescence

Skin sections were incubated with antibodies recognizing BrdU (1:3, Becton Dickinson),

thymine dimer (clone KTM53 (recognizing all cyclobutane dimers), 1:1000, Kamiya

Biomedical Company, Seattle, WA), and p53 (1:300, Santa Cruz, Santa Cruz, CA). One

section per slide was a negative control that was incubated in 3% bovine serum albumin

(Fisher Scientific, Fair Lawn, NJ) in PBS instead of the primary antibody. For BrdU and

cyclobutane dimer immunofluorescence, ethanol fixed, paraffin embedded sections were

used. Slides were incubated in 2N HCl and concentrated Trypsin (Sigma, 1 mg Trypsin

per mL distilled water) for 5 min each. Sections were blocked in 10% goat serum prior to

overnight incubation with the primary antibody. Following primary antibody incubation,

sections were incubated with biotinylated $F(Ab)_2$ fragment goat anti-mouse secondary

antibody (Jackson ImmunoResearch, West Grove, PA), Texas-red Streptavidin (Vector Laboratories, Burlingame, CA), and 4',6-Diamidino-2-Phenylindole (DAPI)-containing mounting media, consisting of 50% glycerol in PBS with 0.01g/mL propyl gallate (Sigma) and 1.5 μg/mL DAPI (Molecular Probes, Invitrogen, Carlsbad, CA). For quantification of immunofluorescence, the investigator was blinded to the identity of the samples. BrdU was quantified by counting BrdU-positive cells and DAPI-positive basal cells at ten randomly selected fields using a 20x objective and the BrdU labeling index is reported as the percentage of BrdU-labeled basal cells. The intensity of cyclobutane dimer labeling was quantified using ImageJ software (http://rsb.info.nih.gov/ij/) to determine the mean pixel intensity. The mean pixel intensity of the background was subtracted from the overall fluorescence for three to five randomly selected regions of each skin section. For p53 immunofluorescence, formalin fixed paraffin embedded sections were used and antigen retrieval was performed through alternating heating and cooling cycles in 0.9% Antigen Unmasking Solution (Vector Laboratories). Sections were blocked in 10% goat serum with 1% non-fat milk (Hy-Vee) prior to overnight incubation with the primary antibody. Following primary antibody incubation, the sections were incubated with Alexa Fluor 488-conjugated secondary antibody (Invitrogen), and DAPI-containing mounting media. p53 labeling was quantified by counting the number of p53-positive cells per p53-positive focus and the number of p53-positive foci per mm skin. Statistics were calculated using a Student's t-test and results were deemed significant for $p \leq 0.05$.

Immunoblotting

Flash frozen whole skin from mice was homogenized using a Tissue Master 125 (OMNI International, Marietta, GA) in lysis buffer containing 10 M Tris (pH 7.4), 150 mM NaCl, 10% glycerol, 1% Triton X-100, 1 mM EDTA, Complete Protease Inhibitor Cocktail (Roche, Mannheim, Germany), 1 mM sodium orthovanadate (Na_3VO_4), 1.5 μM EGTA, and 10 μM sodium fluoride (NaF). Protein was loaded and separated using sodium dodecyl sulfate polyacrylamide gel electrophoresis (SDS-PAGE) gels (Bio-Rad Laboratories) and transferred to nitrocellulose membranes (Bio-Rad Laboratories). The evenness of loading and transfer was determined by Ponceau S staining (Sigma) and by immunoblotting for actin (*in vitro*) or glyceraldehyde 3-phosphate dehydrogenase (GAPDH, *in vivo*). Membranes were blocked with 5% nonfat dry milk (Hy-vee, Des Moines) in PBS, incubated overnight with antibodies recognizing Erbb2 (1:200, Upstate, Temecula, CA), phospho-Erbb2 (Tyrosine 1248, Upstate), proliferating cell nuclear antigen (PCNA, 1:800, Dako, Glostrup, Denmark), GAPDH (1:1000, Novus, Littleton, CO), Actin (1:10,000, Sigma), or Cdc25A (1:500, Santa Cruz), then incubated with horseradish peroxidase-conjugated secondary antibodies (Cell Signaling), and chemiluminescent reagents (Pierce, Rockford, IL) prior to autoradiography. Protein levels were quantified by densitometry using 1DScanEX Software (Scanalytics, Fairfax, VA). Statistics were calculated using a Student's *t*-test and results were deemed significant for $p \leq 0.05$.

Flow Cytometry

Cultured keratinocytes were removed from 60 mm polystyrene dishes after sham- or UV-irradiation using 0.25% Trypsin-EDTA (Invitrogen), incubated with Vindelov's solution (85), containing 3.5 mM Tris base (pH 7.6), 10 mM NaCl, 10 μg/mL Ribonuclease A (Sigma), 75 μg/mL propidium iodide (Sigma), 0.1% Igepal (Sigma), and filtered through 35 μm nylon filters into 5 mL polystyrene round bottom tubes (Becton Dickinson). For flow cytometry using *in vivo* skin samples, three 60 μm sections were cut from formalin-fixed paraffin embedded blocks. The sections were dewaxed with xylene and rehydrated with decreasing concentrations of ethanol (100%, 90%, 70%, 50%, and distilled water). Cells were then digested in 0.05% pepsin (Sigma) in PBS with pH 1.5 and incubated with Vindelov's Solution (85). Flow cytometry analysis was performed in the Creighton Flow Cytometry Core Lab on the FACSCalibur flow cytometer (Becton Dickinson, Franklin Lakes, NJ) using FL2 channel (585-42 bandpass filter). Single cells were identified by measuring area (FL2-A) and width (FL2-W) and data for at least 10,000 singlets for each sample were collected in list mode data files using Cell Quest Pro software (Becton Dickinson). A histogram for FL2-A intensity was plotted for single cells and cell cycle distributions were determined using ModFit LT 3.1 software (Verity Software House, Topsham ME). Statistics were calculated using a Student's *t*-test and results were deemed significant for $p \leq 0.05$.

Chapter 3: Results

Skin-targeted Erbb2 *mutant mice were developed to overcome off-target effects of other models*

To investigate the influence of Erbb2 activation on the response of the skin to UV, a skin-targeted conditional *Erbb2* null (*Erbb2* mutant) mouse was developed. This model was used to test the hypothesis that promotion of S-phase progression by Erbb2 after UV-irradiation limits DNA damage repair and results in increased mutagenesis after chronic UV-irradiation.

To generate *Erbb2* mutant mice, mice with two *Erbb2* floxed alleles (*Erbb2$^{fl/fl}$*) were crossed with mice in which Cre recombinase expression is driven by the Keratin 14 (K14) promoter. In mice, expression of K14 begins in the basal keratinocytes of the epidermis at E14.5 (86), resulting in the expression of Cre recombinase and the genetic ablation of *Erbb2* in the epidermis (Figure 5A). The *Erbb2* mutant mice were healthy and viable (Figure 5B). Immunoblotting confirmed that the average Erbb2 immunoreactivity was reduced approximately 95% in the keratinocytes of *Erbb2* mutant skin (*Erbb2$^{fl/fl}$ cre$^+$*) when compared to Cre-expressing mice that lack *Erbb2* floxed alleles (*Erbb2$^{wt/wt}$ cre$^+$*, Figure 5C).

For the *Erbb2* mutant mice used in the experiments, the genotypes were determined by polymerase chain reaction analysis and confirmed by immunoblotting (as in Figure 6). Littermate controls lacked Cre recombinase expression, but contained both *Erbb2* floxed alleles (*Erbb2$^{fl/fl}$ cre$^-$*). On average, there was a 95% reduction of Erbb2 immunoreactivity in sham-irradiated *Erbb2* mutant mice compared to littermate controls.

A.
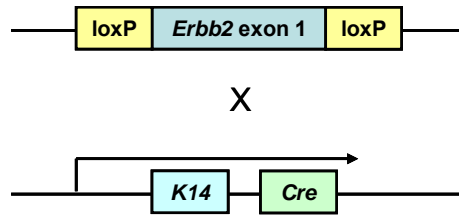
B.

C.
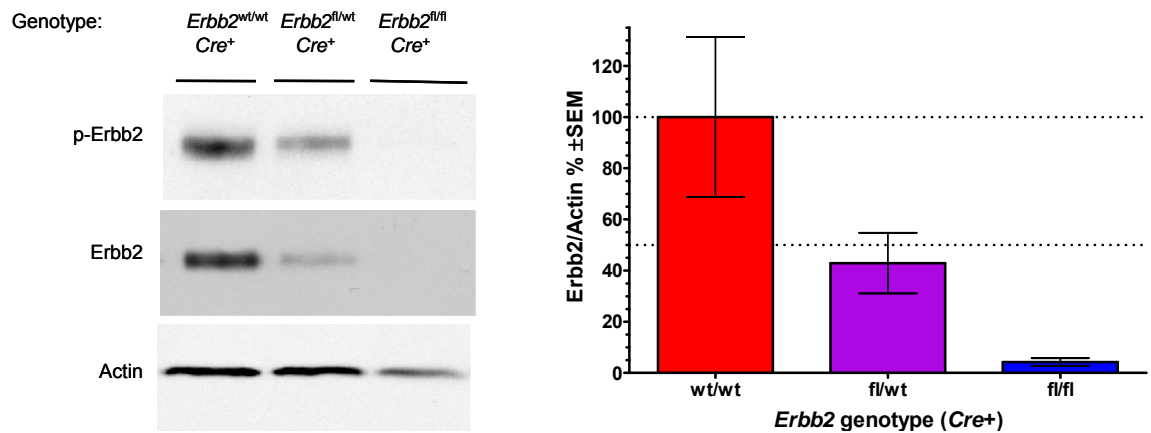
Figure 5. Generation of *Erbb2* mutant mice.

A. *S*kin-targeted conditional *Erbb2* null (*Erbb2* mutant) mouse were generated by crossing *Erbb2$^{fl/fl}$* mice with mice in which expression Cre recombinase is driven by the Keratin 14 (K14) promoter. B. Photograph of an *Erbb2* mutant (*Erbb2$^{fl/fl}$ cre^{+}*) mouse. C. Erbb2 protein immunoreactivity in 8 day old transgenic mice expressing Cre recombinase in the skin (left panel). Quantification utilized densitometry analysis for multiple replicates (described in Materials and Methods, right panel).
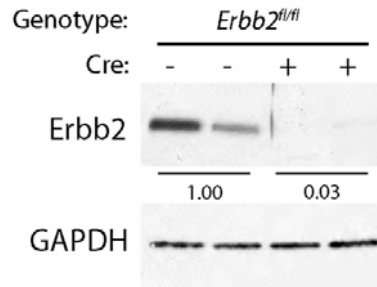
Figure 6. Erbb2 immunoreactivity is decreased in *Erbb2* mutant skin.
Protein lysate from groups of sham-irradiated skin from *Erbb2* mutant mice
(*Erbb2^fl/fl^ cre^+^*) and littermate controls (*Erbb2^fl/fl^ cre^-^*) was used for immunoblotting
(N=2 mice shown). Numbers indicate mean densitometry for the group after
normalizing each sample to GAPDH.

Genetic ablation of **Erbb2** *results in small differences in cell cycle progression after UV-irradiation*

Non-melanoma skin cancer is caused by chronic exposure to UV-irradiation.
Previous research has implicated UV-activated Erbb2 in the suppression of S-phase arrest
after UV-irradiation, which impairs cells' abilities to repair DNA damage or undergo
apoptosis. UV activates Erbb2 both *in vivo* and *in vitro* and in both mouse and human
skin ((79) and Figure 7A and B). To test the hypothesis that the ablation of *Erbb2* results
in an increased S-phase arrest after UV-irradiation, age-matched groups of *Erbb2* mutant
mice and littermate controls (N=25) were exposed to sham- or UV-irradiation, totaling
26 kJ/m^2 (43 exposures, 0.5-3 kJ/m^2 per week) over the course of 39 weeks. Mice did not
develop any visible skin lesions and were euthanized at several timepoints after the final
(1 kJ/m^2) UV exposure. The ultimate goal of this experiment was to investigate Erbb2's
role in the regulation of cell cycle progression, DNA damage repair, and mutagenesis in
chronically UV-exposed skin. The experimental design, including groups of sham- and
UV-irradiated *Erbb2* mutant and littermate controls, is summarized in Figure 8A.

A.   **B.**
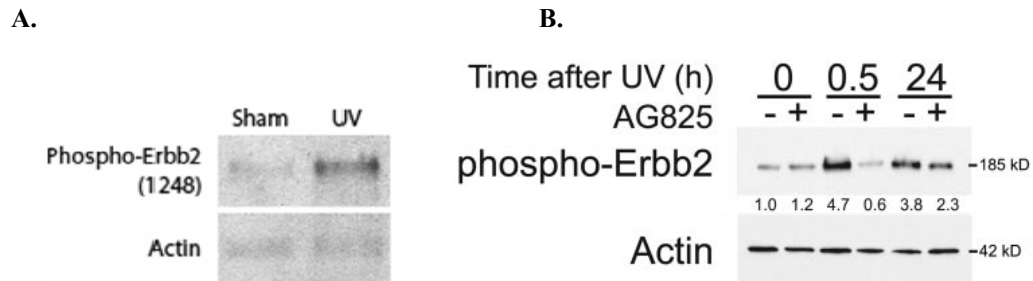
Figure 7. UV-induced activation of Erbb2.

A. Human skin was sham- or UV-irradiated (0.6-1.0 kJ/m^2) and protein lysate for immunoblotting was collected 30 min after UV as described in Materials and Methods. B. Cultured keratinocytes were treated with the Erbb2 inhibitor AG825 and exposed to UV-irradiation (600 J/m^2). Protein lysate for immunoblotting was collected at the indicated timepoints after UV exposure. Numbers indicate mean densitometry for the group after normalizing each sample to actin (reprinted from Am J Pathol 2006;169:1402-1414 with permission from the American Society for Investigative Pathology, (79)).

DNA content flow cytometry was used to determine the cell cycle distribution of keratinocytes in the skin after chronic UV-irradiation (Figure 8B). In skin from both *Erbb2* mutant mice and littermate controls, the percentage of cells in G_0/G_1-phases declined by about 6% in the first 36 h after UV-irradiation (Figure 8B, left panel). This decrease in G_0/G_1-phase cells was associated with a corresponding increase in the percentage of S-phase cells (Figure 8B, middle panel). In *Erbb2* mutant skin, the percentage of S-phase cells increased by about 3% when compared to UV-exposed control skin 12 h after UV-irradiation (Figure 8B, middle panel) with a corresponding decrease in G_2/M-phase cells (Figure 8B, right panel). 18 h after UV-irradiation, there was an increase in G_2/M-phase cells (~2%, Figure 8B, right panel) with a corresponding decrease in G_0/G_1-phase cells (Figure 8B, left panel). The increase in S-phase cells 12 h after UV-irradiation was consistent with the S-phase accumulation seen in keratinocytes treated with AG825 (*in vivo* and *in vitro*, unpublished data) although statistical

significance could not be determined due to insufficient sample size. In addition, at 18 h

after UV-irradiation the percentage of cells in G_2/M phase were significantly increased

(~3.5%, Figure 8B, right panel) and the G_0/G_1-phase cells were significantly decreased

(~2%, Figure 8B, left panel) in *Erbb2* mutant skin compared to littermate controls.

Based on this analysis, small (<5%) but statistically significant differences in cell cycle

progression exist between the control and *Erbb2* mutant mice after UV-irradiation.

A.
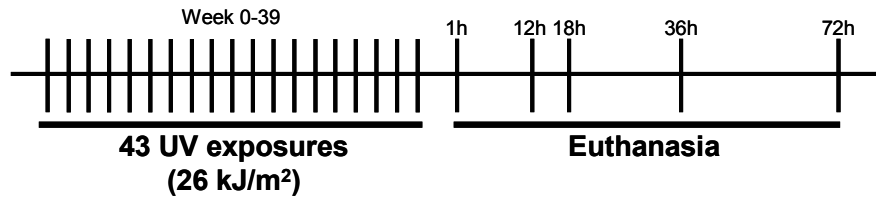
B.
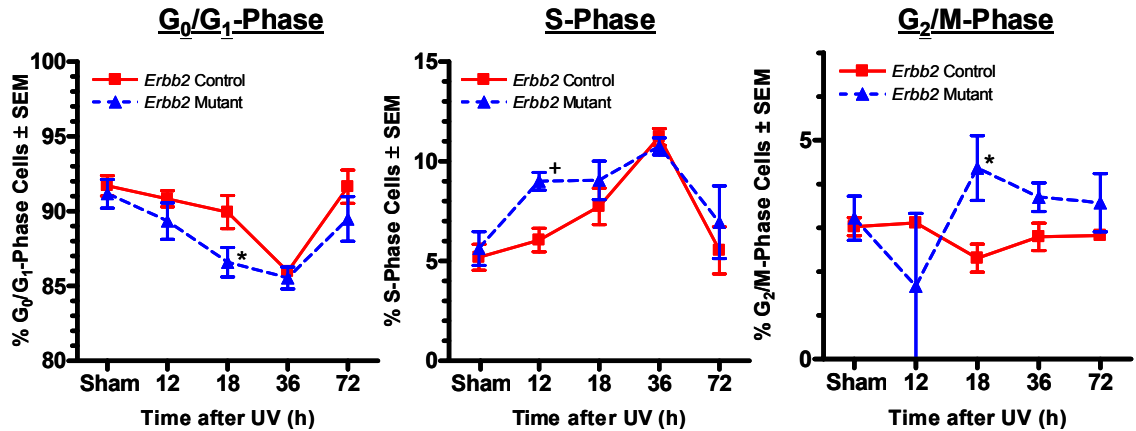
Figure 8. Cell cycle progression from *Erbb2* mutant and littermate controls after receiving 43 UV-exposures totaling 26 kJ/m^2.

Groups of mice were exposed to sham- and UV-irradiated 43 times over a period of 39 weeks (totaling 26 kJ/m^2) and were euthanized at the indicated timepoints. A. Schematic representation of experiment. B. Flow cytometry for DNA content was performed on formalin-fixed paraffin embedded blocks containing sham- and UV-irradiated mouse skin as described in Materials and Methods (N≥3 except 12 h (N=2); * p≤0.05; +, *t*-test could not be performed due to insufficient number of samples).

To determine whether the increase in S-phase cells is due to a cell cycle arrest (as in AG825 treated skin) or increased DNA synthesis, BrdU-labeling was quantified using immunofluorescence. Representative images of BrdU immunofluorescence are shown in Figure 9A. The number of BrdU-positive basal cells and DAPI-labeled basal cells were quantified in photomicrographs like those shown in Figure 9A to obtain the results presented in Figure 9B. In control skin lacking Cre recombinase expression, the number of basal cells undergoing DNA synthesis was increased by 18 h after UV-irradiation (~10%, Figure 9B).

By contrast, in *Erbb2* mutant skin, the percentage of basal cells in which DNA synthesis was occurring increased by 12 h after UV-irradiation (~10%, Figure 9B), though statistical significance could not be determined due to insufficient sample size. These results suggest that in *Erbb2* mutant skin, the increase in S-phase cells observed in the flow cytometry analysis was due to increased DNA synthesis instead of a cell cycle arrest (Figure 9B).

Since an S-phase arrest was not observed in the skin from *Erbb2* mutant mice, similar Cdc25A immunoreactivity was expected in the skin of *Erbb2* mutant mice and littermate controls. As anticipated, Cdc25A immunoreactivity in the *Erbb2* mutant mice was similar to that of the littermate controls after UV-irradiation consistent with normal cell cycle progression (Figure 10). Although the average Cdc25A immunoreactivity in sham-irradiated *Erbb2* mutant skin was reduced the signal for Cdc25A was quite variable in these samples.

In addition, immunoblotting for proliferating cell nuclear antigen (PCNA), a protein involved in DNA synthesis, was performed as another measure of DNA synthesis.

A.

Sham	UV (18 h)

Red: BrdU; Blue: DAPI
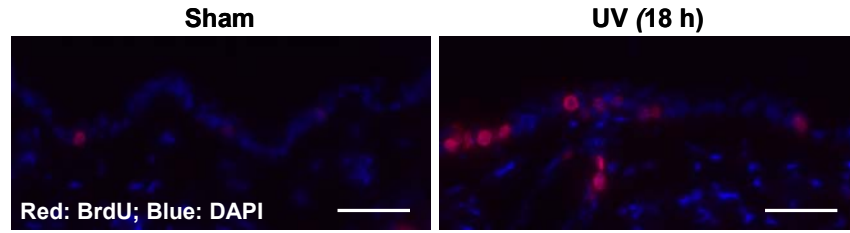
B.
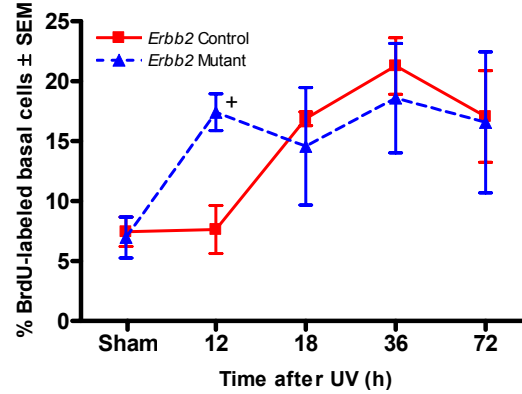
Figure 9. DNA synthesis after UV-irradiation quantified by BrdU labeling index.
Groups of mice were sham- or UV-irradiated (43 exposures totaling 26 kJ/m^2). Mice
were injected with BrdU 1 h prior to euthanization as described in Materials and
Methods. Bromodeoxyuridine (BrdU) immunofluorescence was performed on skin
sections from these mice. A. Representative BrdU immunofluorescence
photomicrographs illustrating the increase in DNA synthesis after UV-irradiation
(scale bar 40 μm). B. Mice injected with BrdU were euthanized at the indicated
timepoints. DNA synthesis was quantified as the percentage of BrdU-labeled basal
cells (N≥3 except 12 h (N=2); * p≤0,05; +, t-test could not be performed due to
insufficient number of samples).

The average PCNA immunoreactivity in skin from *Erbb2* mutant mice was
decreased in sham-irradiated mice and increased 12 h after UV-irradiation when
compared to the littermate controls. The increase in PCNA immunoreactivity 12 h after
UV-irradiation suggests increased DNA synthesis, consistent with the BrdU-
quantification. Taken together, these results demonstrate that genetic ablation of *Erbb2*
using the K14 promoter to drive Cre recombinase expression in an *Erbb2$^{fl/fl}$* murine

27

model does not cause an S-phase arrest after UV-irradiation and DNA synthesis is instead increased 12 h after UV-irradiation.
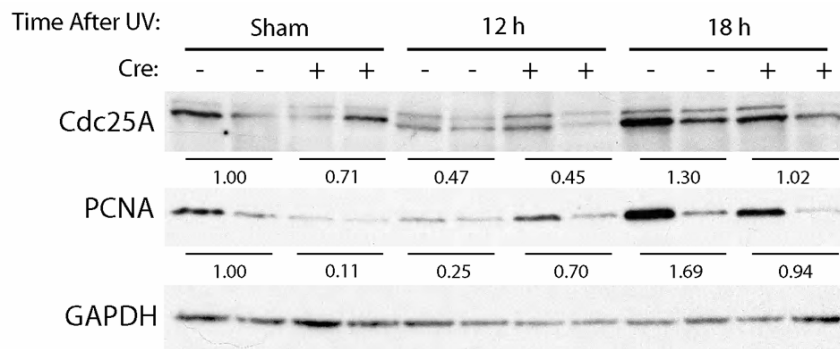
Figure 10. Immunoblotting consistent with normal cell cycle progression.
Groups of mice were exposed to sham- and UV-irradiation (43 exposures totaling 26 kJ/m^2). Protein lysate was extracted from whole skin as described in Materials and Methods. Immunoblotting was performed on protein lysate from *Erbb2* mutant mice and littermate controls euthanized at the indicated timepoints. There were not consistent differences between PCNA and Cdc25A immunoreactivity in skin of *Erbb2* mutant and littermate controls (N=2 mice shown). Numbers indicate mean densitometry for the group after normalizing each sample to GAPDH.

Genetic ablation of **Erbb2** *improves DNA damage repair after UV-irradiation*

One way that a cell protects against mutagenesis is through efficient repair of UV-induced DNA photoproducts, such as cyclobutane dimers (16). Therefore, the repair of cyclobutane dimers was deemed an appropriate measurement for the efficiency of DNA repair and was used to test the hypothesis that Erbb2 reduces the efficiency of DNA damage repair. Since an S-phase arrest was not observed in *Erbb2* mutant skin after UV-irradiation, improved DNA damage repair efficiency was not anticipated.

DNA damage was quantified by measuring the intensity of cyclobutane dimer immunofluorescence with Image J software. Representative images of the cyclobutane

dimer immunofluorescence are shown in Figure 11A. The majority of nuclei in the

epidermis stained positive for cyclobutane dimers by 12 h after UV-irradiation. By 72 h,

staining for cyclobutane dimers was weak, suggesting that UV-induced DNA damage

was mostly repaired within 72 h after UV-irradiation. The intensity of cyclobutane dimer

labeling was quantified in photomicrographs like those shown in Figure 11A to obtain the

results presented in Figure 11B.
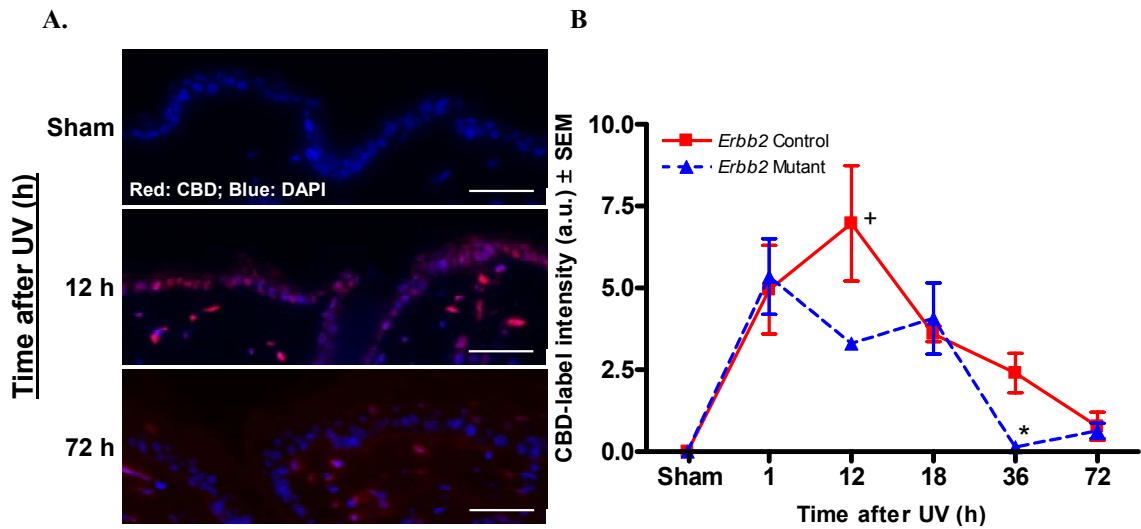
Figure 11. UV-induced DNA damage quantified by cyclobutane dimer immunofluorescence intensity.

Groups of mice were exposed to sham- and UV-irradiation (43 exposures totaling 26 kJ/m^2). Skin sections were mounted on slides and stained for cyclobutane dimers. A. Cyclobutane dimer (CBD) immunofluorescence illustrates formation of DNA damage after UV-irradiation (12 h) and their eventual repair (72 h, scale bars 40 μm). B. DNA damage was quantified by the intensity of cyclobutane dimer staining, as measured using Image J software (described in Materials and Methods, N≥3 except 1h and 12 h (N=2), a.u. arbitrary units; * p≤0.05; +, *t*-test could not be performed due to insufficient number of samples).

Cyclobutane dimers were detected 1 h after UV-irradiation. Reduction of

cyclobutane dimer-labeling intensity began by 12 h and 18 h after UV-irradiation in skin

from *Erbb2* mutant and littermate controls, respectively. The average cyclobutane dimer

immunofluorescence intensity 36 h after UV-irradiation in the *Erbb2* mutant was similar to that of sham-irradiated skin, suggesting that DNA damage was fully repaired (Figure 11B). In control skin lacking Cre recombinase expression, cyclobutane dimer-label intensity was not fully reduced until 72 h after UV-irradiation (Figure 11B). These results suggest that DNA damage repair occurs more quickly in the skin of *Erbb2* mutant mice indicating improved efficiency. However, these results are surprising given that no S-phase arrest was observed in *Erbb2* mutant skin after sham- or UV-irradiation.

p53-positive foci are smaller in UV-irradiated skin from Erbb2 *mutant mice*

Trp53 mutations are the most common earliest known mutations in non-melanoma skin cancer, occurring in 12-58% of SCC and BCC (20). Previous reports have documented the association of *Trp53* mutations with an increased half-life of the protein in UV-exposed mouse skin (24-29). In addition, p53 immunostaining has been used to quantify UV-induced mutagenesis and predict the cancer risk in normal and chronically UV exposed skin (87-89). The vast majority of UV-induced skin tumors in mouse skin are SCC (90), ~50% of which contain p53 mutations (reviewed in (91)). UV-induced *ras* mutations occurs in SCC at a lower percentage rate (10-20%) though chemically induced skin tumors (i.e. di-methyl-benzanthracene (DMBA)/ 12-O-tetradecanoylphorbol-13-acetate (TPA)) are ras-dependent (reviewed in (91)). *p16/CDKN2A* mutations occur in about 24% of SCC (92) and *PTCH* deletion occurs in about 70% BCC but not commonly SCC (reviewed in (91)). Therefore, quantification of mutant p53 was used to test the hypothesis that genetic ablation of *Erbb2* results in decreased mutagenesis. Although an increased S-phase arrest after UV-irradiation was

not detected in skin from *Erbb2* mutant mice compared to littermate controls, decreased

mutagenesis could result from the improved DNA damage repair efficiency observed in

Erbb2 mutant skin.

A.

Green: p53; Blue: DAPI
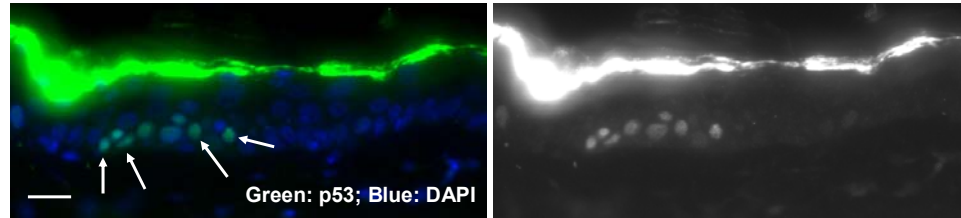
B.
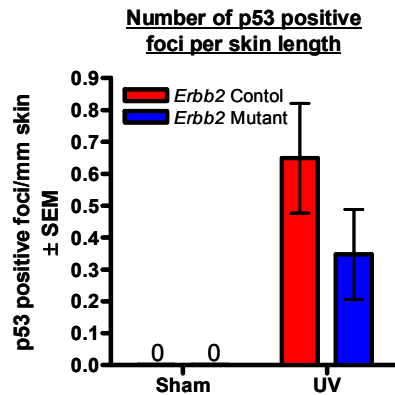
C.
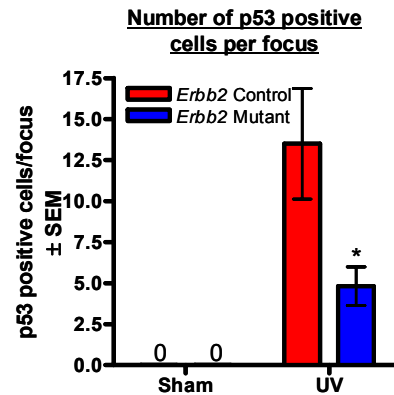
Figure 12. Mutagenesis quantified by p53 immunofluorescence.
Groups of mice were exposed to sham- and UV-irradiation (43 exposures totaling
26 kJ/m^2). Skin sections were mounted on slides and stained for p53. A.
Representative images of p53 immunofluorescence after UV-irradiation (arrows
indicate several p53 positive cells, scale bar 20 μm). B. Nuber of p53 positive foci
per mm skin. There was no statistically significance difference between groups
(N=11 mice). C. Number of p53 positive cells per focus (* p≤0.05).

p53 immunofluorescence was performed on sham- and UV-irradiated skin from

Erbb2 mutant mice and littermate controls. p53 visible by immunofluorescence was

assumed to be mutant p53 because wild type p53 usually has a short half-life and cannot

be detected by immunofluorescence. p53-labeled cells were found in clusters (foci)

originating in the basal layers of the epidermis suggesting clonal expansion of a single

cell (Figure 12A). p53 was localized to the nucleus in all cells that stained positive for p53.

Results from mice euthanized between 12 h and 72 h after UV-irradiation were combined in the analysis which included the number of p53-positive foci per unit skin length and average number of p53-positive cells per p53-positive focus. Though the average number of p53-positive foci was decreased in *Erbb2* mutant skin by about 50%, there was not a statistically significant difference between the skin from *Erbb2* mutant mice and littermate controls (Figure 12B). Interestingly, the number of cells per p53-positive focus was significantly decreased in skin from *Erbb2* mutant mice compared to littermate controls (~65%, Figure 12C). This result suggests that Erbb2 promotes proliferation of keratinocytes containing mutant p53.

Erbb2 *mutant mice may adapt to loss of Erbb2 by maintaining Cdc25A*

The discovery that genetic ablation of *Erbb2* does not result in the S-phase arrest observed after treatment with AG825 or transfection with an Erbb2-targeted siRNA (Figure 8B and unpublished data) led to an investigation into the cause of these inconsistencies. First, to ensure that the lack of a substantial cell cycle difference was not unique to the *in vivo* mouse model, DNA content flow cytometry was performed on cultured keratinocytes from *Erbb2* mutant mice and littermate controls after sham- and UV-irradiation (Figure 13). Similar to the *in vivo* model, an increase in S-phase arrest was not observed in UV-irradiated *Erbb2* mutant keratinocytes in culture (Figure 13, middle panel). Contrary to our hypothesis, *Erbb2* mutant cells display decreased S-phase cells 18 h after UV-irradiation (Figure 13, middle panel) and increased G_0/G_1-phase cells 22 h after UV-irradiation compared to littermate controls (Figure 13, left panel). The

absence of a large difference in cell cycle progression led to an investigation into why the cell cycle profile in *Erbb2* mutant skin is similar to that of littermate controls.

One possible explanation for the absence of an S-phase arrest is that cells lacking Erbb2 compensate for its loss. Since expression of K14 and therefore genetic abrogation of *Erbb2* begins at E14.5 (86), it is possible that compensation occurs during the life of the study, or perhaps even by birth. In order to test this possibility $Erbb2^{fl/fl}$ keratinocytes in culture were infected with a Cre recombinase adenovirus which reduced Erbb2 immunoreactivity by about 95% (Figure 14). Empty (control) and Cre recombinase virus-infected keratinocytes were exposed to sham- or UV-irradiation 24 h after infection and the cell cycle profile was analyzed using flow cytometry (Figure 15).
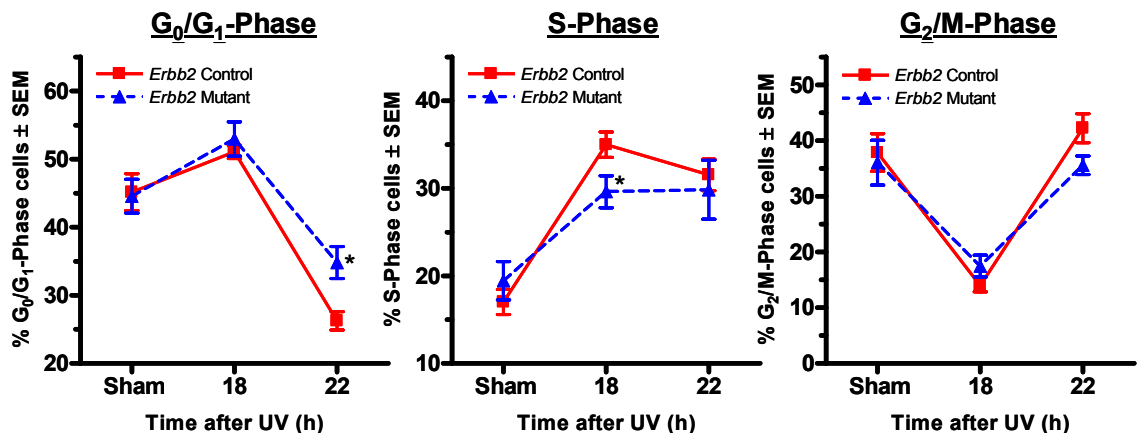
Figure 13. Flow cytometry analysis of cultured keratinocytes from *Erbb2* mutant mice and littermate controls.

Keratinocytes cultured from *Erbb2* mutant and littermate controls were exposed to sham- or UV-irradiation (600 J/m^2). Cells were collected for flow cytometry at the indicated timepoints and analyzed for DNA content (N=4 dishes, * p≤0.05).

In empty virus-infected keratinocytes there was a decrease in G_0/G_1-phase cells (~18%, Figure 15, left panel) with a corresponding increase in S-phase (~10%, Figure 15, middle panel) and G_2/M-phase cells (~8%, Figure 15,

right panel) 22 h after UV-irradiation. In Cre recombinase virus-infected cells there was an increase in S-phase cells (~20%, Figure 15, middle panel) with a corresponding decrease in G_2/M-phase cells (~20%, Figure 15, right panel) 22 h after UV-irradiation. The S-phase accumulation in the Cre recombinase
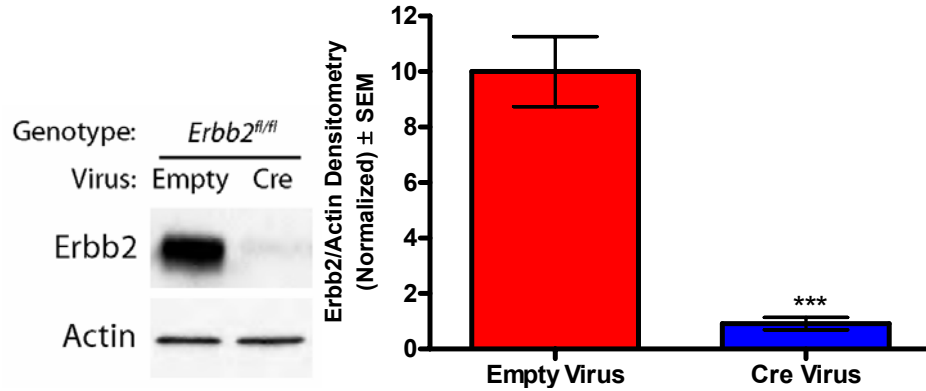
Figure 14. Cre recombinase infection of *Erbb2^{fl/fl}* keratinocytes reduces Erbb2 immunoreactivity.

Cultured keratinocytes from *Erbb2^{fl/fl} cre⁻* mice were infected with an empty or Cre adenovirus. Immunoblotting was performed on protein lysates from sham-irradiated keratinocytes (left panel). The bar graph (right panel) illustrates Erbb2 immunoreactivity based on multiple replicates (N=5 dishes, *** $p \leq 0.001$).
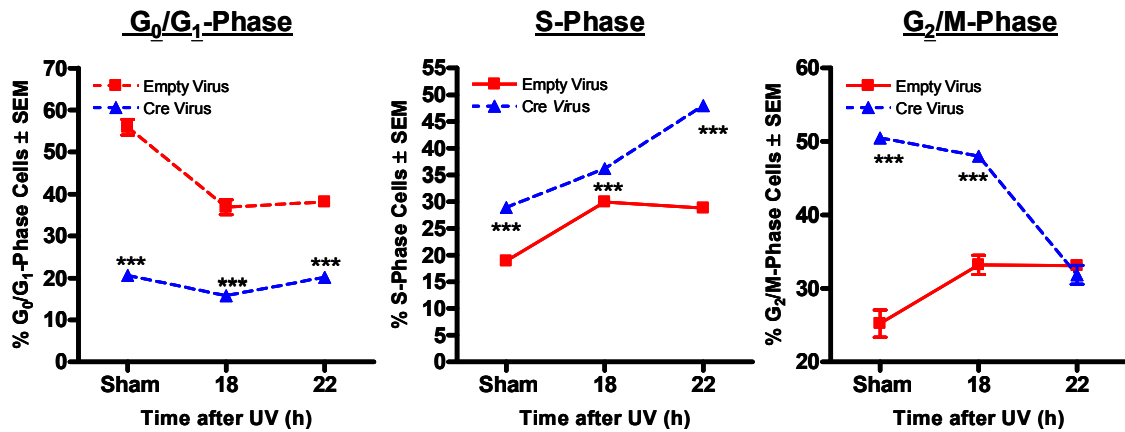
Figure 15. Flow cytometry analysis of virus-infected *Erbb2^{fl/fl}* keratinocytes.
Cultured keratinocytes from *Erbb2^{fl/fl}* Cre⁻ mice were infected with an empty or Cre adenovirus. DNA content flow cytometry analysis was performed on sham- or UV-irradiation (600 J/m^2) virus-infected keratinocytes at the indicated timepoints (N=4 dishes, *** $p \leq 0.001$).

virus-infected keratinocytes is likely due to a cell cycle arrest instead of increased DNA

synthesis since it corresponds to a decrease in the following cell cycle phase (G_2/M).

However, BrdU quantification should be performed to exclude the possibility of

increased DNA synthesis.

A.
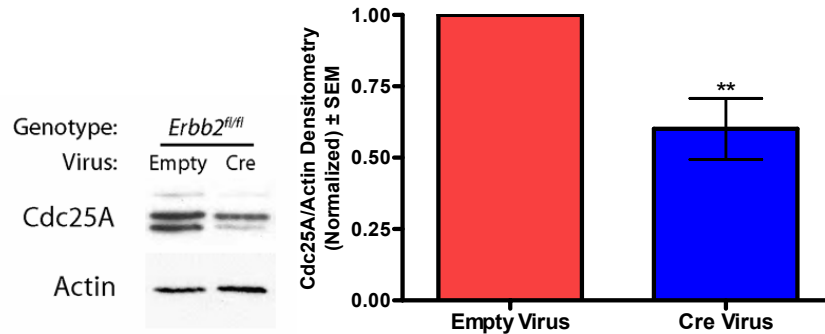
B.
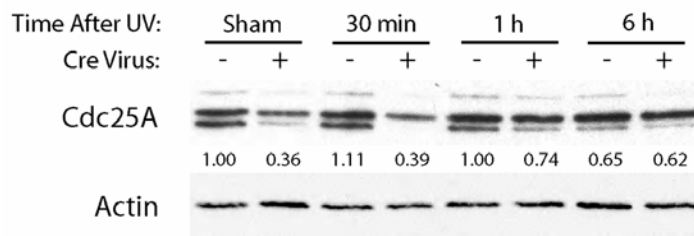
Figure 16. Cdc25A immunoreactivity in Cre recombinase virus-infected *Erbb2$^{fl/fl}$* and *Erbb2* mutant keratinocytes.

Keratinocytes were cultured from *Erbb2$^{fl/fl}$ cre$^-$* and *Erbb2* mutant mice.   Groups of cultured keratinocytes from *Erbb2$^{fl/fl}$ cre$^-$* mice were infected with an empty or Cre recombinase adenovirus (A, B). A. Protein lysate was collected for immunoblotting (left panel). The bar graph illustrates average Cdc25A immunoreactivity after based on multiple replicates (right panel, N=10 dishes, ** p≤0.01). B. Virus-infected keratinocytes were exposed to UV-irradiation (600 J/m^2) and protein lysates were collected and used for immunoblotting at the indicated timepoints (representative of 2 immunoblots with similar results). Numbers indicate densitometry after normalizing each sample to GAPDH.

Since Cdc25A is a regulator of CDK2 and the progression through S-phase,

Cdc25A immunoreactivity in sham- and UV-irradiated keratinocytes was examined to

determine whether reduced Cdc25A levels could be responsible for the high percentage

of S-phase cells in sham-irradiated, Cre recombinase virus-infected keratinocytes.

Cdc25A immunoreactivity was decreased in Cre recombinase virus-infected cells after

sham- and UV-irradiation (up to 1 h after UV, Figure 16A and B). However, in sham-

irradiated keratinocytes from *Erbb2* mutant mice, there was no difference in Cdc25A

immunoreactivity (Figure 17). These results suggest that *Erbb2* mutant cells compensate

for loss of Erbb2 by maintaining Cdc25A protein levels.
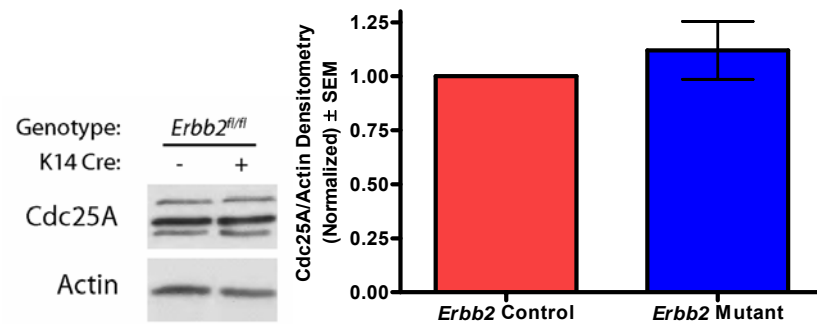
Figure 17. Cdc25A immunoreactivity in *Erbb2* mutant keratinocytes.
Protein lysate was collected from sham-irradiated keratinocytes from *Erbb2* mutant
mice and littermate controls for immunoblotting (Left panel). The bar graph
illustrates average Cdc25A immunoreactivity based on multiple replicates (N=5
dishes). There are no statistically significant differences between these groups.

Chapter 4: Discussion

Erbb2 is an important player in the diversification and potency of Erbb signaling. The overexpression of Erbb2 in several internal cancers is associated with chemotherapy resistance and a poor prognosis. The importance of Erbb2 in internal cancers has been confirmed by the development and success of Erbb2-targeted therapeutic options. Most studies focus on Erbb2's role in cells that overexpress Erbb2 as opposed to those that express the protein at normal physiological levels. However, our research suggests that repeated activation of Erbb2 following UV-irradiation could be responsible for producing similar oncogenic results in the skin.

Previous studies in our lab have demonstrated that Erbb2 is activated through an indirect mechanism after UV-irradiation and promotes cell cycle progression. These experiments suggested that Erbb2 could regulate the ATR DNA damage pathway by maintaining Cdc25A, thereby promoting cell cycle progression and preventing S-phase arrest. We have also demonstrated that inhibition of Erbb2 resulted in decreased skin tumorigenesis after chronic UV-exposure, providing further evidence of Erbb2's role in promoting UV-induced non-melanoma skin cancer. However, these studies were performed using either an inhibitor or siRNA, both of which commonly produce off-target effects. In order to eliminate off-target effects, a skin-targeted conditional *Erbb2* null (*Erbb2* mutant) mouse was developed in which Erbb2 expression was ablated in the epithelial cells of the skin. This new model was designed to eliminate off-target effects and to test the hypothesis that promotion of S-phase progression by Erbb2 after UV-irradiation limits DNA damage repair and results in increased mutagenesis.

Cell cycle analysis using the *Erbb2* mutant model produced some unexpected results. In contrast to our previous results from Erbb2 inhibitor treated and UV-exposed mice, DNA synthesis and S-phase progression were actually increased in UV-exposed *Erbb2* mutant skin when compared to UV-exposed control mice. Similar analyses performed using *Erbb2* mutant keratinocytes in culture produced a similar response. Consistent with the lack of cell cycle arrest upon genetic ablation of *Erbb2*, Cdc25A was not significantly reduced in keratinocytes from *Erbb2* mutant mice.

These results led us to investigate the inconsistencies between the *Erbb2* mutant and AG825 inhibitor models. Experiments were performed in which the floxed *Erbb2* alleles were ablated by infection of cultured keratinocytes with a Cre recombinase expressing virus. This allowed us to examine the immediate effects of *Erbb2* ablation. Sham- and UV-irradiated Cre recombinase virus-infected keratinocytes produced an S-phase arrest similar to that observed in inhibitor treated keratinocytes and skin. This model for ablation of *Erbb2* expression paralleled the timing of the inhibitor experiments and allowed us to examine the effects of *Erbb2* ablation within the first 48 h after the receptor's signaling was reduced. In addition, Cdc25A immunoreactivity was reduced in sham- and UV-irradiated keratinocytes following viral Cre recombinase expression consistent with the S-phase arrest observed in inhibitor and siRNA treated cells and skin. Because results from the inhibitor and virus infection models are obtained within 48 h of Cre recombinase virus infection or Erbb2 inhibitor treatment, we hypothesize that keratinocytes compensate for prolonged loss of Erbb2 through the maintenance of Cdc25A. Experiments are ongoing in the lab to test this hypothesis.

In addition to the cell cycle analyses, the effects of Erbb2 on repair of UV-induced DNA damage and mutagenesis were also assessed. Although no increase in cell cycle arrest was documented in *Erbb2* mutant skin, the efficiency of UV-induced DNA damage repair in *Erbb2* mutant skin was improved. Quantification of cyclobutane dimers revealed that DNA damage in *Erbb2* mutant skin was repaired within 36 h after UV-irradiation, while damage in skin from littermate controls was not fully repaired until 72 h after UV-irradiation. Because the more rapid DNA damage repair observed in *Erbb2* mutant skin cannot be contributed to a cell cycle arrest, Erbb2's role in reducing the efficiency of nucleotide excision repair appears to involve a mechanism independent of its regulation of the cell cycle. To determine how Erbb2 might be involved in the regulation of nucleotide excision repair, analyses involving the repair factors involved in nucleotide excision repair should be performed in *Erbb2* mutant mice.

As in the analysis of DNA repair efficiency, a significant difference in the size or number of p53-positive foci between *Erbb2* mutant and littermate controls was not expected due to the lack of an effect of *Erbb2* ablation on cell cycle arrest *in vivo*. Surprisingly, however, the size of p53-positive foci was significantly reduced in UV-exposed *Erbb2* mutant skin when compared to littermate controls. We hypothesize that this is the result of decreased clonal expansion of cells containing *Trp53* mutations. First, to confirm that p53-positive foci actually contain mutant p53, *Trp53* should be sequenced in normal keratinocytes, in cells from p53-positive foci in UV-exposed skin, and in UV-induced skin tumors. Sequencing *Trp53* will also confirm clonal expansion and existence of UV-signature mutations (C→T or CC→TT transitions). The first sequencing targets should be *Trp53* codons 270 and 275 , which are the most common UV-induced *Trp53*

mutations in mouse skin and at which pyrimidine dimers are known to form (93). p53

should also be analyzed after fewer UV exposures when p53-positive foci would likely

be smaller and more distinct to ensure that p53-positive foci are not overlapping.

An analysis of the role of Erbb2 in the cell cycle progression, DNA damage

repair, survival, and proliferation of keratinocytes with mutant p53 may prove interesting.

It has previously been demonstrated that wild type p53 reduces HER2 (Erbb2)-induced

proliferation in cells that overexpress HER2. Wild type p53 promotes cell cycle arrest

and apoptosis, while mutant p53 promotes HER2-induced proliferation and cell cycle

progression in HER2 overexpressing cells (94). To determine whether p53 has a

regulatory role in cells containing normal physiological levels of Erbb2, mutant

(dominant negative) and wild type p53 should be introduced into cells with or without

Erbb2 and analyses quantifying DNA damage repair, survival, and proliferation should

be performed. In addition, the effect of modulating Erbb2 in cells with *Trp53* mutations

should be investigated. In addition, we intend to perform double immunofluorescence

with p53 and PCNA to determine whether cells with p53 mutations are rapidly

proliferating.

Although our results are somewhat preliminary, the data presented herein suggest

that a strategy for administering an Erbb2 inhibitor to prevent UV induced skin

carcinogenesis might be effective if applied using a schedule that intermittently blocks

Erbb2 signaling. Currently, the only available preventative treatment for UV-induced

non-melanoma skin cancer is sunscreen which either absorbs, reflects or scatters UV rays

(reviewed in (95)). However, full protection for the entire UVA and UVB spectrum to

which we are exposed (290-400 nm) is not commercially available. Erbb2/HER2 is

activated in human and mouse skin 30 min after UV-irradiation as measured by phospho-Erbb2 immunoreactivity (Figure 7). An improved preventative treatment would be particularly beneficial for immunosuppressed patients that have an increased risk for UV-related skin cancer.

Though the *Erbb2* mutant model does not directly support the idea of Erbb2 inhibition as a skin cancer preventative, experiments using the Erbb2 inhibitor and Cre recombinase virus-infected *Erbb2*$^{fl/fl}$ keratinocytes do suggest that a short term inhibitor of Erbb2 kinase function might be effective. The development of an effective Erbb2-targeted inhibitor treatment would require the demonstration that prolonged loss of Erbb2 causes compensatory upregulation of Cdc25A and increased proliferation after UV-exposure. The most likely treatment regime, supported by experiments using the Erbb2 inhibitor and Cre recombinase virus infection of *Erbb2*$^{fl/fl}$ cells, would be one in which Erbb2 is intermittently inhibited prior to UV-exposure to avoid prolonged Erbb2 inhibition and potential drug resistance. In addition, it will be important to confirm the mechanism in which Erbb2 regulates the ATR pathway in response to UV-irradiation. The targeting of a signaling protein downstream of Erbb2 might provide an effective therapeutic option while reducing the risk of serious side effects (i.e. cardiotoxicity) and drug resistance.

In order to further investigate the potential compensatory mechanism upon prolonged Erbb2 loss, a number of additional analyses are indicated. First, to determine whether the lack of an S-phase arrest is due to maintenance of Cdc25A, DNA content flow cytometry should be analyzed in sham- and UV-irradiated, Cre recombinase virus-infected cells in which Cdc25A levels have been increased by transfection with a

Cdc25A plasmid. If the maintenance of Cdc25A is responsible for the compensatory mechanism after genetic ablation of Erbb2, the increase of Cdc25A should repair the cell cycle defect in Cre infected cells. In addition, Cdc25A immunoreactivity should be analyzed in sham-irradiated, Cre recombinase virus-infected keratinocytes to determine the timeline in which Cdc25A is recovered after loss of Erbb2. A comparable *in vivo* experiment would require the development of transgenic mice in which Cre recombinase expression targeted to the skin is conditionally expressed (i.e. tamoxifen-induced expression as described in (96)). This would allow us to observe the effects of UV-irradiation after short term loss of *Erbb2* and determine the timeline in which a compensatory mechanism is developed. The ability to reduce Erbb2 in adult mice would also allow us to determine whether a compensatory mechanism occurs in during adulthood or only when Erbb2 is lost early in development when there is increased plasticity. These experiments will provide guidance for determining an appropriate treatment schedule for an Erbb2-targeted skin cancer preventative.

The mechanism through which Cdc25A is recovered after loss of Erbb2 should be investigated. If Erbb2 regulates maintenance of Cdc25A through the inhibition of Chk1 by the PI3K/Akt pathway (Figure 4), it is possible that other RTKs activate this pathway. EGFR, like Erbb2, is activated after UV-irradiation and has been demonstrated to promote UV-induced skin tumorigenesis (97). UV-irradiation induced activation of EGFR results in the activation of the PI3K/Akt pathway through heterodimerization with Erbb3 or association with adapter proteins (i.e. Gab1, Cbl (97-100)). Though the Erbb2-Erbb3 pathway is more potent (101), the EGFR-Erbb3 heterodimer is also able to activate this pathway. Erbb3 has six direct binding sites for the p85 subunit of PI3K, making it

the preferred Erbb receptor for initiating this signaling cascade (102-104). Since it has been suggested that incomplete inhibition of HER3 (Erbb3) in Herceptin-treated patients results in a cell's ability to resist treatment (70;105), it is reasonable to consider that Erbb3 might be involved in the compensatory mechanism in *Erbb2* mutant skin. However, preliminary data from an unrelated experiment suggests that there are not significant differences in EGFR and Erbb3 activation between sham-irradiated skin from *Erbb2* mutant and littermate controls (*in vivo*, unpublished data). Therefore, other proteins capable of activating the PI3K/Akt pathway should be considered.

Currently, a tumor experiment is underway to determine the influence of genetic ablation of *Erbb2* on UV-induced skin carcinogenesis. The purpose of this experiment is to compare the time until tumor development, tumor multiplicity, incidence, volume, and stage in *Erbb2* mutant mice and littermate controls following chronic UV-irradiation. Based on the results presented in this report, the improved DNA damage repair and decreased clonal expansion of cells with *Trp53* mutations after UV-irradiation of *Erbb2* mutant skin should translate to decreased mutagenesis and delayed skin tumor development compared to skin from littermate controls. The additional analyses proposed here would provide further insight into the potential outcome of this experiment.

The results presented in this report suggest that cells lacking Erbb2 recover Cdc25A, which may be responsible for the absence of an S-phase arrest after sham-and UV-irradiation in *Erbb2* mutant skin when compared to the models using Cre recombinase viral infection, Erbb2 inhibition, and Erbb2-targeted siRNA transfection. A role for Erbb2 has also been implicated as a regulator of DNA repair mechanisms and

43

clonal expansion of cells with mutant p53. Because the improved DNA damage repair and increased mutagenesis cannot be attributed to an S-phase arrest, Erbb2 likely regulates these processes through mechanisms independent of its regulation of cell cycle progression.

Bibliography

(1) Lechler T, Fuchs E. Asymmetric cell divisions promote stratification and differentiation of mammalian skin. Nature 2005 Sep 8;437(7056):275-80.

(2) De Gruijl FR. Photocarcinogenesis: UVA vs. UVB radiation. Skin Pharmacol Appl Skin Physiol 2002 Sep;15(5):316-20.

(3) Sancar A, Lindsey-Boltz LA, Unsal-Kacmaz K, Linn S. Molecular mechanisms of mammalian DNA repair and the DNA damage checkpoints. Annu Rev Biochem 2004;73:39-85.

(4) Abraham RT. Cell cycle checkpoint signaling through the ATM and ATR kinases. Genes Dev 2001 Sep 1;15(17):2177-96.

(5) Zou L, Elledge SJ. Sensing DNA damage through ATRIP recognition of RPA-ssDNA complexes. Science 2003 Jun 6;300(5625):1542-8.

(6) Sinha RP, Hader DP. UV-induced DNA damage and repair: a review. Photochem Photobiol Sci 2002 Apr;1(4):225-36.

(7) Shechter D, Costanzo V, Gautier J. Regulation of DNA replication by ATR: signaling in response to DNA intermediates. DNA Repair (Amst) 2004 Aug;3(8-9):901-8.

(8) Falck J, Mailand N, Syljuasen RG, Bartek J, Lukas J. The ATM-Chk2-Cdc25A checkpoint pathway guards against radioresistant DNA synthesis. Nature 2001 Apr 12;410(6830):842-7.

(9) Mailand N, Falck J, Lukas C, Syljuasen RG, Welcker M, Bartek J, et al. Rapid destruction of human Cdc25A in response to DNA damage. Science 2000 May 26;288(5470):1425-9.

(10) Busino L, Chiesa M, Draetta GF, Donzelli M. Cdc25A phosphatase: combinatorial phosphorylation, ubiquitylation and proteolysis. Oncogene 2004 Mar 15;23(11):2050-6.

(11) Gabrielli BG, De Souza CP, Tonks ID, Clark JM, Hayward NK, Ellem KA. Cytoplasmic accumulation of cdc25B phosphatase in mitosis triggers centrosomal microtubule nucleation in HeLa cells. J Cell Sci 1996 May;109 (Pt 5):1081-93.

(12) Lammer C, Wagerer S, Saffrich R, Mertens D, Ansorge W, Hoffmann I. The cdc25B phosphatase is essential for the G2/M phase transition in human cells. J Cell Sci 1998 Aug;111 (Pt 16):2445-53.

(13) Millar JB, Blevitt J, Gerace L, Sadhu K, Featherstone C, Russell P. p55CDC25 is a nuclear protein required for the initiation of mitosis in human cells. Proc Natl Acad Sci U S A 1991 Dec 1;88(23):10500-4.

(14) Xiao Z, Chen Z, Gunasekera AH, Sowin TJ, Rosenberg SH, Fesik S, et al. Chk1 mediates S and G2 arrests through Cdc25A degradation in response to DNA-damaging agents. J Biol Chem 2003 Jun 13;278(24):21767-73.

(15) Koundrioukoff S, Polo S, Almouzni G. Interplay between chromatin and cell cycle checkpoints in the context of ATR/ATM-dependent checkpoints. DNA Repair (Amst) 2004 Aug;3(8-9):969-78.

(16) Brash DE. UV mutagenic photoproducts in Escherichia coli and human cells: a molecular genetics perspective on human skin cancer. Photochem Photobiol 1988 Jul;48(1):59-66.

(17) Pfeifer GP, You YH, Besaratinia A. Mutations induced by ultraviolet light. Mutat Res 2005 Apr 1;571(1-2):19-31.

(18) Pfeifer GP. p53 mutational spectra and the role of methylated CpG sequences. Mutat Res 2000 May 30;450(1-2):155-66.

(19) Ikehata H, Ono T. Significance of CpG methylation for solar UV-induced mutagenesis and carcinogenesis in skin. Photochem Photobiol 2007 Jan;83(1):196-204.

(20) Missero C, D'Errico M, Dotto GP, Dogliotti E. The Molecular Basis of Skin Carcinogenesis. In: Coleman WB, Tsongalis GJ, editors. The Molecular Basis of Human Cancer.Totowa: Humana Press; 2002. p. 407-26.

(21) Seemann S, Maurici D, Olivier M, de Fromentel CC, Hainaut P. The tumor suppressor gene TP53: implications for cancer management and therapy. Crit Rev Clin Lab Sci 2004;41(5-6):551-83.

(22) Brash DE, Rudolph JA, Simon JA, Lin A, McKenna GJ, Baden HP, et al. A role for sunlight in skin cancer: UV-induced p53 mutations in squamous cell carcinoma. Proc Natl Acad Sci USA 1991;88:10124-8.

(23) Ziegler A, Leffell DJ, Kunala S, Sharma HW, Gailani M, Simon JA, et al. Mutation hotspots due to sunlight in the p53 gene of nonmelanoma skin cancers. Proc Natl Acad Sci USA 1993;90:4216-20.

(24) Strano S, Dell'Orso S, Di AS, Fontemaggi G, Sacchi A, Blandino G. Mutant p53: an oncogenic transcription factor. Oncogene 2007 Apr 2;26(15):2212-9.

(25) Cadwell C, Zambetti GP. The effects of wild-type p53 tumor suppressor activity and mutant p53 gain-of-function on cell growth. Gene 2001 Oct 17;277(1-2):15-30.

(26) Midgley CA, Lane DP. p53 protein stability in tumour cells is not determined by mutation but is dependent on Mdm2 binding. Oncogene 1997 Sep 4;15(10):1179-89.

(27) Haupt Y, Maya R, Kazaz A, Oren M. Mdm2 promotes the rapid degradation of p53. Nature 1997 May 15;387(6630):296-9.

(28) Buschmann T, Minamoto T, Wagle N, Fuchs SY, Adler V, Mai M, et al. Analysis of JNK, Mdm2 and p14(ARF) contribution to the regulation of mutant p53 stability. J Mol Biol 2000 Jan 28;295(4):1009-21.

(29) Sigal A, Rotter V. Oncogenic mutations of the p53 tumor suppressor: the demons of the guardian of the genome. Cancer Res 2000 Dec 15;60(24):6788-93.

(30) Housman TS, Feldman SR, Williford PM, Fleischer AB, Jr., Goldman ND, Acostamadiedo JM, et al. Skin cancer is among the most costly of all cancers to treat for the Medicare population. J Am Acad Dermatol 2003 Mar;48(3):425-9.

(31) Chen JG, Fleischer AB, Jr., Smith ED, Kancler C, Goldman ND, Williford PM, et al. Cost of nonmelanoma skin cancer treatment in the United States. Dermatol Surg 2001 Dec;27(12):1035-8.

(32) Yuspa SH. The pathogenesis of squamous cell cancer: lessons learned from studies of skin carcinogenesis--Thirty-third G.H.A. Clowes Memorial Award Lecture. Cancer Res 1994;54:1178-89.

(33) Glick A, Ryscavage A, Perez-Lorenzo R, Hennings H, Yuspa S, Darwiche N. The high-risk benign tumor: evidence from the two-stage skin cancer model and relevance for human cancer. Mol Carcinog 2007 Aug;46(8):605-10.

(34) Tyrrell RM. Activation of mammalian gene expression by the UV component of sunlight- -from models to reality. Bioessays 1996 Feb;18(2):139-48.

(35) Herrlich P, Sachsenmaier C, Radler-Pohl A, Gebel S, Blattner C, Rahmsdorf HJ. The mammalian UV response: mechanism of DNA damage induced gene expression. Adv Enzyme Regul 1994;34:381-95.

(36) Sachsenmaier C, Radler-Pohl A, Muller A, Herrlich P, Rahmsdorf HJ. Damage to DNA by UV light and activation of transcription factors. Biochem Pharmacol 1994 Jan 13;47(1):129-36.

(37) Koch-Paiz CA, Amundson SA, Bittner ML, Meltzer PS, Fornace AJ, Jr. Functional genomics of UV radiation responses in human cells. Mutat Res 2004 May 18;549(1-2):65-78.

(38) Euvrard S, Kanitakis J, Claudy A. Skin cancers after organ transplantation. N Engl J Med 2003 Apr 24;348(17):1681-91.

(39) Knebel A, Rahmsdorf HJ, Ullrich A, Herrlich P. Dephosphorylation of receptor tyrosine kinases as target of regulation by radiation, oxidants or alkylating agents. EMBO J 1996 Oct 1;15(19):5314-25.

(40) Huang RP, Wu JX, Fan Y, Adamson ED. UV activates growth factor receptors via reactive oxygen intermediates. J Cell Biol 1996 Apr;133(1):211-20.

(41) Gross S, Knebel A, Tenev T, Neininger A, Gaestel M, Herrlich P, et al. Inactivation of protein-tyrosine phosphatases as mechanism of UV-induced signal transduction. J Biol Chem 1999 Sep 10;274(37):26378-86.

(42) Hashimoto K, Higashiyama S, Asada H, Hashimura E, Kobayashi T, Sudo K, et al. Heparin-binding epidermal growth factor-like growth factor is an autocrine

growth factor for human keratinocytes. J Biol Chem 1994 Aug 5;269(31):20060-6.

(43) Brown SB, Krause D, Ellem KA. Low fluences of ultraviolet irradiation stimulate HeLa cell surface aminopeptidase and candidate "TGF alpha ase" activity. J Cell Biochem 1993 Jan;51(1):102-15.

(44) Massague J, Pandiella A. Membrane-anchored growth factors. Annu Rev Biochem 1993;62:515-41.

(45) Schechter AL, Hung MC, Vaidyanathan L, Weinberg RA, Yang-Feng TL, Francke U, et al. The neu gene: an erbB-homologous gene distinct from and unlinked to the gene encoding the EGF receptor. Science 1985 Sep 6;229(4717):976-8.

(46) Coussens L, Yang-Feng TL, Liao YC, Chen E, Gray A, McGrath J, et al. Tyrosine kinase receptor with extensive homology to EGF receptor shares chromosomal location with neu oncogene. Science 1985 Dec 6;230(4730):1132-9.

(47) Semba K, Kamata N, Toyoshima K, Yamamoto T. A v-erbB-related protooncogene, c-erbB-2, is distinct from the c-erbB-1/epidermal growth factor-receptor gene and is amplified in a human salivary gland adenocarcinoma. Proc Natl Acad Sci U S A 1985 Oct;82(19):6497-501.

(48) Akiyama T, Sudo C, Ogawara H, Toyoshima K, Yamamoto T. The product of the human c-erbB-2 gene: a 185-kilodalton glycoprotein with tyrosine kinase activity. Science 1986 Jun 27;232(4758):1644-6.

(49)   Di Fiore PP, Pierce JH, Kraus MH, Segatto O, King CR, Aaronson SA. erbB-2 is

a potent oncogene when overexpressed in NIH/3T3 cells. Science 1987 Jul

10;237(4811):178-82.

(50)   Yarden Y, Sliwkowski MX. Untangling the ErbB signalling network. Nat Rev

Mol Cell Biol 2001 Feb;2(2):127-37.

(51)   Olayioye MA, Neve RM, Lane HA, Hynes NE. The ErbB signaling network:

receptor heterodimerization in development and cancer. EMBO J 2000 Jul

3;19(13):3159-67.

(52)   Guy PM, Platko JV, Cantley LC, Cerione RA, Carraway KL, III. Insect cell-

expressed p180erbB3 possesses an impaired tyrosine kinase activity. Proc Natl

Acad Sci U S A 1994 Aug 16;91(17):8132-6.

(53)   Graus-Porta D, Beerli RR, Daly JM, Hynes NE. ErbB-2, the preferred

heterodimerization partner of all ErbB receptors, is a mediator of lateral signaling.

EMBO J 1997 Apr 1;16(7):1647-55.

(54)   Karunagaran D, Tzahar E, Beerli RR, Chen X, Graus-Porta D, Ratzkin BJ, et al.

ErbB-2 is a common auxiliary subunit of NDF and EGF receptors: implications

for breast cancer. EMBO J 1996 Jan 15;15(2):254-64.

(55)   Jones JT, Akita RW, Sliwkowski MX. Binding specificities and affinities of egf

domains for ErbB receptors. FEBS Lett 1999 Mar 26;447(2-3):227-31.

(56)   Baulida J, Kraus MH, Alimandi M, Di Fiore PP, Carpenter G. All ErbB receptors

other than the epidermal growth factor receptor are endocytosis impaired. J Biol

Chem 1996 Mar 1;271(9):5251-7.

(57) Lenferink AE, Pinkas-Kramarski R, Van de Poll ML, Van Vugt MJ, Klapper LN, Tzahar E, et al. Differential endocytic routing of homo- and hetero-dimeric ErbB tyrosine kinases confers signaling superiority to receptor heterodimers. EMBO J 1998 Jun 15;17(12):3385-97.

(58) Schlessinger J. Cell signaling by receptor tyrosine kinases. Cell 2000;103(2):211-25.

(59) Rebay I. Keeping the receptor tyrosine kinase signaling pathway in check: lessons from Drosophila. Dev Biol 2002 Nov 1;251(1):1-17.

(60) Marmor MD, Skaria KB, Yarden Y. Signal transduction and oncogenesis by ErbB/HER receptors. Int J Radiat Oncol Biol Phys 2004 Mar 1;58(3):903-13.

(61) Madson JG, Hansen LA. Multiple mechanisms of Erbb2 action after ultraviolet irradiation of the skin. Mol Carcinog 2007 Aug;46(8):624-8.

(62) Lee KF, Simon H, Chen H, Bates B, Hung MC, Hauser C. Requirement for neuregulin receptor erbB2 in neural and cardiac development. Nature 1995 Nov 23;378(6555):394-8.

(63) Lin W, Sanchez HB, Deerinck T, Morris JK, Ellisman M, Lee KF. Aberrant development of motor axons and neuromuscular synapses in erbB2- deficient mice. Proc Natl Acad Sci U S A 2000 Feb 1;97(3):1299-304.

(64) Morris JK, Lin W, Hauser C, Marchuk Y, Getman D, Lee KF. Rescue of the cardiac defect in ErbB2 mutant mice reveals essential roles of ErbB2 in peripheral nervous system development. Neuron 1999 Jun;23(2):273-83.

(65) Chan R, Hardy WR, Laing MA, Hardy SE, Muller WJ. The catalytic activity of the ErbB-2 receptor tyrosine kinase is essential for embryonic development. Mol Cell Biol 2002 Feb;22(4):1073-8.

(66) Ozcelik C, Erdmann B, Pilz B, Wettschureck N, Britsch S, Hubner N, et al. Conditional mutation of the ErbB2 (HER2) receptor in cardiomyocytes leads to dilated cardiomyopathy. Proc Natl Acad Sci U S A 2002 Jun 25;99(13):8880-5.

(67) Crone SA, Zhao YY, Fan L, Gu Y, Minamisawa S, Liu Y, et al. ErbB2 is essential in the prevention of dilated cardiomyopathy. Nat Med 2002 May;8(5):459-65.

(68) Valabrega G, Montemurro F, Aglietta M. Trastuzumab: mechanism of action, resistance and future perspectives in HER2-overexpressing breast cancer. Ann Oncol 2007 Jun;18(6):977-84.

(69) Bengala C, Zamagni C, Pedrazzoli P, Matteucci P, Ballestrero A, Da PG, et al. Cardiac toxicity of trastuzumab in metastatic breast cancer patients previously treated with high-dose chemotherapy: a retrospective study. Br J Cancer 2006 Apr 10;94(7):1016-20.

(70) Hsieh AC, Moasser MM. Targeting HER proteins in cancer therapy and the role of the non-target HER3. Br J Cancer 2007 Aug 20;97(4):453-7.

(71) Lebeau S, Masouye I, Berti M, Augsburger E, Saurat JH, Borradori L, et al. Comparative analysis of the expression of ERBIN and Erb-B2 in normal human skin and cutaneous carcinomas. Br J Dermatol 2005 Jun;152(6):1248-55.

(72) Stoll SW, Kansra S, Peshick S, Fry DW, Leopold WR, Wiesen JF, et al. Differential utilization and localization of ErbB receptor tyrosine kinases in skin

compared to normal and malignant keratinocytes. Neoplasia 2001 Jul;3(4):339-50.

(73) Bol D, Kiguchi K, Beltran L, Rupp T, Moats S, Gimenez-Conti I, et al. Severe follicular hyperplasia and spontaneous papilloma formation in transgenic mice expressing the neu oncogene under the control of the bovine keratin 5 promoter. Mol Carcinog 1998 Jan;21(1):2-12.

(74) Xie W, Wu X, Chow LT, Chin E, Paterson AJ, Kudlow JE. Targeted expression of activated erbB-2 to the epidermis of transgenic mice elicits striking developmental abnormalities in the epidermis and hair follicles. Cell Growth Differ 1998 Apr;9(4):313-25.

(75) Xie W, Chow LT, Paterson AJ, Chin E, Kudlow JE. Conditional expression of the ErbB2 oncogene elicits reversible hyperplasia in stratified epithelia and up-regulation of TGFalpha expression in transgenic mice. Oncogene 1999 Jun 17;18(24):3593-607.

(76) Kiguchi K, Bol D, Carbajal S, Beltran L, Moats S, Chan K, et al. Constitutive expression of erbB2 in epidermis of transgenic mice results in epidermal hyperproliferation and spontaneous skin tumor development. Oncogene 2000 Aug 31;19(37):4243-54.

(77) Baojun L, Haitao Z, Shuqin L, Wei C, Runjiang L. The Expression of C-erbB-1 nd C-erbB-2 oncogenes in basal cell carcinom nd squamous cell carcinoma of skin. Chin Med Sci J 1996 Jun;11(2):106-9.

(78) Krahn G, Leiter U, Kaskel P, Udart M, Utikal J, Bezold G, et al. Coexpression patterns of EGFR, HER2, HER3 and HER4 in non-melanoma skin cancer. Eur J Cancer 2001 Jan;37(2):251-9.

(79) Madson JG, Lynch DT, Tinkum KL, Putta SK, Hansen LA. Erbb2 regulates inflammation and proliferation in the skin after ultraviolet irradiation. Am J Pathol 2006 Oct;169(4):1402-14.

(80) Puc J, Keniry M, Li HS, Pandita TK, Choudhury AD, Memeo L, et al. Lack of PTEN sequesters CHK1 and initiates genetic instability. Cancer Cell 2005 Feb;7(2):193-204.

(81) King FW, Skeen J, Hay N, Shtivelman E. Inhibition of Chk1 by activated PKB/Akt. Cell Cycle 2004 May;3(5):634-7.

(82) Leu M, Bellmunt E, Schwander M, Farinas I, Brenner HR, Muller U. Erbb2 regulates neuromuscular synapse formation and is essential for muscle spindle development. Development 2003 Jun;130(11):2291-301.

(83) Hennings H. Primary culture of keratinocytes from newborn mouse epidermis in medium with lowered levels of Ca^{2+}. In: Leigh I, Watt FM, editors. Keratinocyte Methods.Cambridge, UK: Cambridge University Press; 1994. p. 21-3.

(84) Fisher GJ, Datta SC, Talwar HS, Wang ZQ, Varani J, Kang S, et al. Molecular basis of sun-induced premature skin ageing and retinoid antagonism. Nature 1996 Jan 25;379(6563):335-9.

(85) Vindelov LL. Flow microfluorometric analysis of nuclear DNA in cells from solid tumors and cell suspensions. A new method for rapid isolation and straining of nuclei. Virchows Arch B Cell Pathol 1977 Aug 10;24(3):227-42.

(86) Byrne C, Tainsky M, Fuchs E. Programming gene expression in developing epidermis. Development 1994;120(9):2369-83.

(87) Nakazawa H, English D, Randell PL, Nakazawa K, Martel N, Armstrong BK, et al. UV and skin cancer: specific p53 gene mutation in normal skin as a biologically relevant exposure measurement. Proc Natl Acad Sci USA 1994;91:360-4.

(88) Rebel H, Kram N, Westerman A, Banus S, van Kranen HJ, De Gruijl FR. Relationship between UV-induced mutant p53 patches and skin tumours, analysed by mutation spectra and by induction kinetics in various DNA-repair-deficient mice. Carcinogenesis 2005 Dec;26(12):2123-30.

(89) De Gruijl FR. p53 mutations as a marker of skin cancer risk: comparison of UVA and UVB effects. Exp Dermatol 2002;11 Suppl 1:37-9.

(90) Trempus CS, Mahler JF, Ananthaswamy HN, Loughlin SM, French JE, Tennant RW. Photocarcinogenesis and susceptibility to UV radiation in the v-Ha-ras transgenic Tg.AC mouse. J Invest Dermatol 1998 Sep;111(3):445-51.

(91) Boukamp P. Non-melanoma skin cancer: what drives tumor development and progression? Carcinogenesis 2005 Oct;26(10):1657-67.

(92) Soufir N, Moles JP, Vilmer C, Moch C, Verola O, Rivet J, et al. P16 UV mutations in human skin epithelial tumors. Oncogene 1999 Sep 23;18(39):5477-81.

(93) You YH, Szabo PE, Pfeifer GP. Cyclobutane pyrimidine dimers form preferentially at the major p53 mutational hotspot in UVB-induced mouse skin tumors. Carcinogenesis 2000 Nov;21(11):2113-7.

(94) Casalini P, Botta L, Menard S. Role of p53 in HER2-induced proliferation or apoptosis. J Biol Chem 2001 Apr 13;276(15):12449-53.

(95) Palm MD, O'Donoghue MN. Update on photoprotection. Dermatol Ther 2007 Sep;20(5):360-76.

(96) Vasioukhin V, Degenstein L, Wise B, Fuchs E. The magical touch: genome targeting in epidermal stem cells induced by tamoxifen application to mouse skin. Proc Natl Acad Sci U S A 1999 Jul 20;96(15):8551-6.

(97) El Abaseri TB, Fuhrman J, Trempus C, Shendrik I, Tennant RW, Hansen LA. Chemoprevention of UV light-induced skin tumorigenesis by inhibition of the epidermal growth factor receptor. Cancer Res 2005 May 1;65(9):3958-65.

(98) Engelman JA, Cantley LC. The role of the ErbB family members in non-small cell lung cancers sensitive to epidermal growth factor receptor kinase inhibitors. Clin Cancer Res 2006 Jul 15;12(14 Pt 2):4372s-6s.

(99) Soltoff SP, Cantley LC. p120cbl is a cytosolic adapter protein that associates with phosphoinositide 3-kinase in response to epidermal growth factor in PC12 and other cells. J Biol Chem 1996 Jan 5;271(1):563-7.

(100) Wan YS, Wang ZQ, Shao Y, Voorhees JJ, Fisher GJ. Ultraviolet irradiation activates PI 3-kinase/AKT survival pathway via EGF receptors in human skin in vivo. Int J Oncol 2001 Mar;18(3):461-6.

(101) Pinkas-Kramarski R, Soussan L, Waterman H, Levkowitz G, Alroy I, Klapper L, et al. Diversification of Neu differentiation factor and epidermal growth factor signaling by combinatorial receptor interactions. EMBO J 1996 May 15;15(10):2452-67.

(102) Prigent SA, Gullick WJ. Identification of c-erbB-3 binding sites for phosphatidylinositol 3'-kinase and SHC using an EGF receptor/c-erbB-3 chimera. EMBO J 1994 Jun 15;13(12):2831-41.

(103) Soltoff SP, Carraway KL, III, Prigent SA, Gullick WG, Cantley LC. ErbB3 is involved in activation of phosphatidylinositol 3-kinase by epidermal growth factor. Mol Cell Biol 1994 Jun;14(6):3550-8.

(104) Hellyer NJ, Cheng K, Koland JG. ErbB3 (HER3) interaction with the p85 regulatory subunit of phosphoinositide 3-kinase. Biochem J 1998 Aug 1;333 (Pt 3):757-63.

(105) Sergina NV, Rausch M, Wang D, Blair J, Hann B, Shokat KM, et al. Escape from HER-family tyrosine kinase inhibitor therapy by the kinase-inactive HER3. Nature 2007 Jan 25;445(7126):437-41.